MASTERARBEIT / MASTER'S THESIS

Titel der Masterarbeit / Title of the Master's Thesis

„Pathogenesis of GFAPα meningo-encephalomyelitis: retrospective cohort study of paired CSF-autopsy patient samples"

verfasst von / submitted by

Sofie Oberndorfer, BSc

angestrebter akademischer Grad / in partial fulfilment of the requirements for the degree of

Magistra pharmaciae (Mag.pharm.)

Wien, 2022 / Vienna 2022

Declaration of authorship:

I hereby certify that the master thesis I am submitting is entirely my own original work except otherwise indicated. I am aware of the University's regulations concerning plagiarism, including those regulations concerning disciplinary actions that may result from plagiarism. Any use of the works of any other author, in any form, is properly acknowledged at their point of use.

Furthermore, I assure (printed and electronic) copies I have submitted are identical.

Acknowledgements

Abstract

Background: Glial fibrillary acidic protein (GFAP) meningo-encephalomyelitis is a novel autoimmune disorder of the CNS associated with IgG autoantibodies against GFAP, an intracellular astrocytic antigen. Until now, only few monocentric case series have been described and the pathogenesis remains widely unclear.

Objectives: To search for autopsy cases with GFAP meningo-encephalomyelitis and to investigate whether the tissue-based assay optimized for anti-neuronal surface antibodies (anti-neuronal TBA) is useful to screen for anti-GFAPα autoantibodies.

Methods: Patient samples (CSF, serum and/or plasma) paired with autopsies or astrocyte-staining in the anti-neuronal TBA were screened for anti-GFAPα autoantibodies using a fixed CBA. Clinical, epidemiological, and neuropathological data were retrospectively obtained and evaluated.

Results: 599 samples of 450 patients (F:M ratio=1.2:1; <19years=2%, 19-65years=33%, >65years=65%) were screened for anti-GFAPα autoantibodies. Neuropathological diagnosis included Creutzfeldt-Jakob disease (222/450), neurodegenerative diseases (66/450), primary neoplasia (e.g., CNS tumors) (30/450), antibody-associated autoimmune encephalitis (20/450), viral infections (7/450), encephalitis (11/450), meningo-encephalitis (6/450), meningitis (2/450), meningo-encephalomyelitis (2/450) and others (85/450). None of the 599 samples were positive for anti-GFAPα autoantibodies. Subsequently, 31 patients with astrocyte-staining in the anti-neuronal TBA were screened for anti-GFAPα autoantibodies. Only one case showed a positive result in the CBA.

Conclusion: Continuous screening for anti-GFAPα autoantibodies in larger autopsy cohorts will be necessary to identify GFAP meningo-encephalomyelitis cases. The anti-neuronal TBA may show unspecific labeling of astrocytes and is therefore not useful for the screening of anti-GFAPα autoantibodies. The establishment of a novel TBA will be necessary to provide a robust second detection method for the confirmation of anti-GFAPα autoantibodies.

List of abbreviations

AD	Alzheimer disease
AIE	autoimmune encephalitis
ALS	amyotrophic lateral sclerosis
AMPAR	α-amino-3-hydroxy-5-methyl-4-isoxazolepropionic acid receptor
ANA	anti-nuclear antibody
ANNA-1	antineuronal nuclear antibodies type 1
ANNA-2	antineuronal nuclear antibodies type 2
APC	antigen presenting cell
AQP4	aquaporin 4
Aqua dist.	distilled water
BBB	blood-brain-barrier
BSA	bovine serum albumin
CASPR2	contactin-associated protein-2
CBA	cell-based assay
CNS	central nervous system
CNTF	ciliary neutrophic factor
CNTN1	Contactin-1
CSF	cerebrospinal fluid
CT-1	cardiotropin-1
CXCL13	chemokine (C-X-C motif) ligand 13
DAB	3,3'-diaminobenzidine
DAPI	4´,6-diamidino-2-phenylindole
DMEM	Dulbecco's Modified Eagle's medium
DNA	desoxyribonucleic acid
EBV	Epstein-Barr-virus
EDTA	ethylenediaminetetraacetic acid
FBS	fetal bovine serum
FDG-PET	2-fluor-2-desoxy-D-glucose positron-emission-tomography
GFAP	glial fibrillary acidic protein
GFP	green fluorescent protein
gp130	glycoprotein 130

GME	granulomatous meningo-encephalomyelitis
HEK	human embryonic kidney cells
HIV	human immunodeficiency virus
HRP	horseradish peroxidase
HSE	Herpes simplex encephalitis
i.v.	intravenous
IF	immunofluorescence
IFA	immunofluorescence assay
IgG	immunoglobulin G
IgLON5	immunoglobulin-like cell adhesion molecule 5
IHC	immunohistochemistry
IVIG	intravenous immunoglobulin
JAK	just another kinase
LIF	leukemia inhibitory factor
LGI1	leucine rich glioma inactivated 1
MERS	mild encephalitis/encephalopathy with splenial lesion syndrome
MOG	Myelin Oligodendrocyte Glycoprotein
MOG-AD	Myelin Oligodendrocyte Glycoprotein antibody associated disease
MRI	magnetic resonance imaging
MS	Multiple sclerosis
NLE	necrotizing leukoencephalitis
NMDAR	N-methyl-D-aspartate receptor
NME	necrotizing meningo-encephalitis
NMO	Neuromyelitis optica
NMOSD	Neuromyelitis optica spectrum disorders
NNO	Neuritis nervi optici
NPC	Division of Neuropathology and Neurochemistry
PCA-1	Purkinje cell antibodies type 1
PDL	poly D-Lysine
Pen-Strep	penicillin-streptomycin
PFA	paraformaldehyde
PML	Progressive multifocal leukoencephalopathy
PNS	Paraneoplastic neurological syndrome

POMS	pediatric-onset multiple sclerosis
PRR	pattern recognition receptor
rpm	rounds per minute
RT	room temperature
r.t.u.	ready to use
STAT	signal transducers and activators of transcription
TBE	Tick-borne encephalitis
UV	ultraviolet

Table of contents

1 Introduction

1.1 Autoimmunity

Autoimmune diseases are caused by an immune response that is misdirected against a human's own cells, tissues, or organs. Approximately seven to nine percent of the population, mostly women, suffer from autoimmune diseases. Over 80 disorders are described to be based on autoimmune responses, while their pathogenesis appears heterogeneously [1]. The severity of these diseases can range from low levels of self-reactivity to intermediate levels and to severe pathological manifestations. They can be either organ-specific, e.g. type I diabetes, or systemic, e.g. systemic lupus erythematosus [2].

A healthy immune system has mechanisms to ensure that lymphocytes do not attack their own molecules, proteins, and cells. The innate immune system uses the Pattern Recognition Receptors (PRRs), while the adaptive immune system uses immunological self-tolerance, leading to the inactivation, elimination and alteration of receptors or to the regulation by regulatory T cells [3]. If these mechanisms fail, the immune response can be directed against self-antigens, leading to autoimmunity and autoimmune diseases [4].

Under physiological conditions, the blood-brain-barrier (BBB) prevents the infiltration of pathogens, erythrocytes, or neurotoxins into the brain. Additionally, the BBB provides a tightly regulated transport system in and out of the central nervous system (CNS) that is essential for a healthy neuronal function. In case of impairment, which can be caused by systemic inflammation, injuries, infection, neurodegenerative diseases, and in this master thesis project most relevantly autoimmune diseases, the permeability of the BBB increases [5]. A higher permeability of the BBB ensures cytokines and other inflammatory mediators as well as CD4$^+$ T cells and other peripheral leukocytes to pass through this barrier and elicit an immune response, which is illustrated in **Figure 1** [6]. This increase in permeability also means that autoreactive immune cells can penetrate through the BBB causing neuroinflammatory diseases, such as multiple sclerosis (MS), neuromyelitis optica (NMO) and antibody-associated autoimmune encephalitis (AIE) [5].
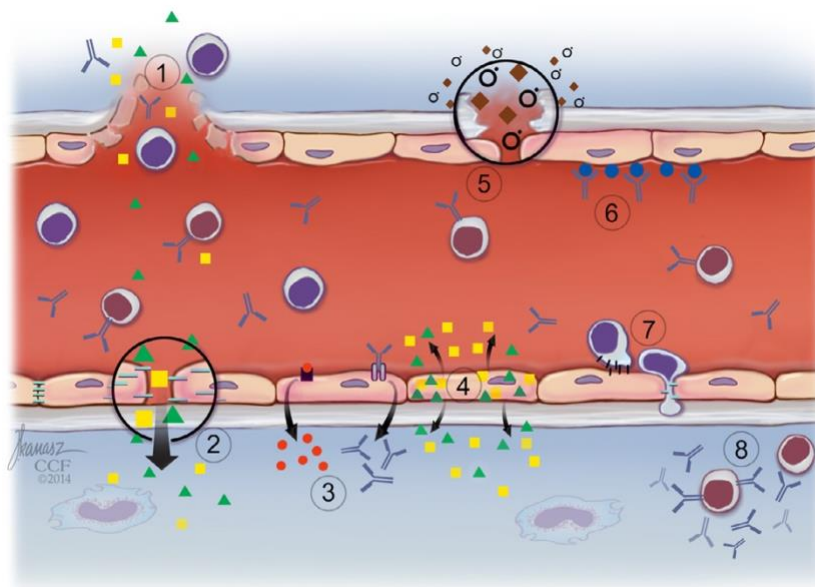
Figure 1: Different mechanisms of inflammatory mediators passaging through the blood-brain barrier. **(1)** shows a vessel rupture that leads to the leakage of cytokines, (auto)antibodies, and (auto)reactive leukocytes. **(2)** illustrates increased paracellular permeability caused by modulation of interendothelial junctions, **(3)** transcellular permeability mediated by increased transporter activity, **(4)** secretion of cytokines (yellow squares) and chemokines (green triangles) by activated endothelial cells, **(5)** degradation of basement membranes and interendothelial junctions caused by radicals, **(6)** antibodies binding antigens on the luminal side of activated endothelial cells, **(7)** enhanced leukocyte trafficking caused by increased expression of leukocyte adhesion molecules and chemokines, and **(8)** intrathecal production of autoantibodies. Copyright: B. Obermeier, A. Verma, and R. M. Ransohoff, "Chapter 3 - The blood–brain barrier," in *Handbook of Clinical Neurology*, vol. 133, S. J. Pittock and A. Vincent, Eds. Elsevier, 2016**.**

1.1.1   Antibody-associated autoimmune encephalitis (AIE)

Antibody-associated AIE describes an inflammatory CNS disorder, which is characterized by the detection of autoantibodies in patient's CSF and/or serum that are directed against specific antigens [7]. It comprises a heterogenous group of immune-associated diseases that exhibit different pathophysiological mechanisms depending on the localization of the antigen and its interaction with the autoantibody [8].

Antibody-associated AIE can broadly be divided into two main groups, which are illustrated in **Figure 2** (classification criteria 2004 [9]): (1) Autoantibodies targeting intracellular neuronal antigens such as cytoplasmic, nuclear, or internal synaptic proteins (see **Figure 2A)**, some of them occur in the setting of a paraneoplastic neurological syndrome (PNS) and are called well-characterized onconeuronal antibodies [8]. These autoantibodies show little or no evidence for direct pathogenicity and inflammation seems to be mediated by cytotoxic T cell infiltration resulting in prominent irreversible

2

neuronal cell loss and therefore patient response to (immuno)therapy is usually poor [7][10]. (2) Autoantibodies targeting extracellular neuronal cell surface or synaptic antigens (see **Figure 2B)** that mediate reversible neuronal dysfunction and cause relatively little neuronal cell death [7][11][12]. They are occasionally associated with cancer, depending on the specific autoantibody, and patients' usually respond well to immunotherapy [13][14].

In 2021, Graus et al. postulated an updated diagnostic criteria for PNS, in which these autoantibodies are no longer classified into the localization of their targeting cell structures, but according to their "risk phenotypes" depending on whether an underlying tumor is present or not: (1) high-risk autoantibodies (>70%), (2) intermediate-risk autoantibodies (30%-70%), and (3) lower-risk autoantibodies (<30%) [15].
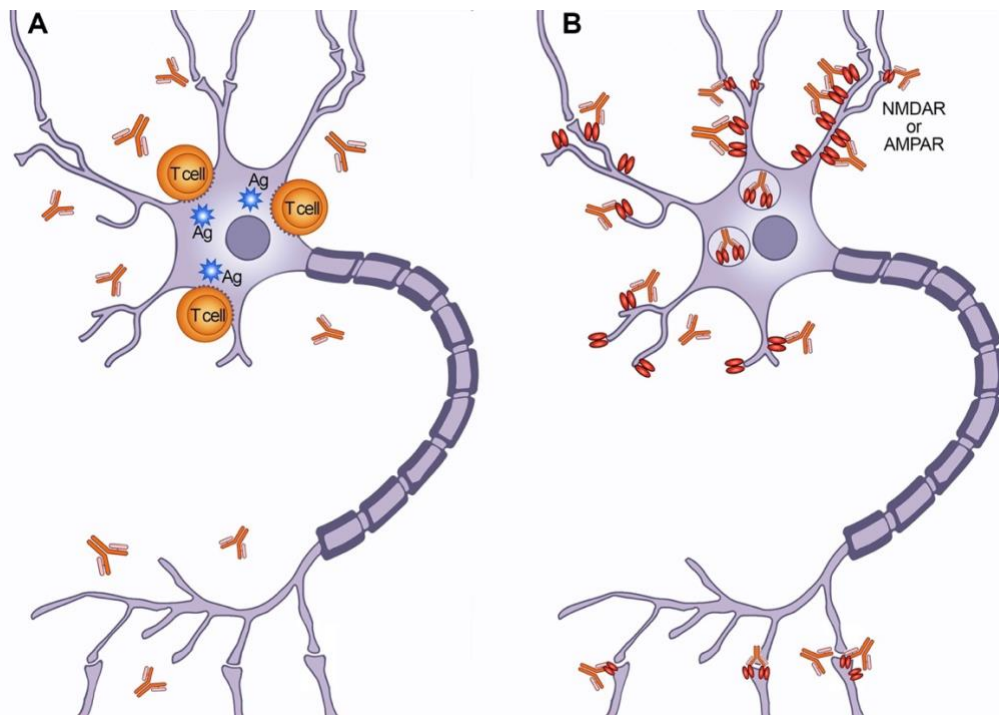
Figure 2: Types of antibody-associated AIE. **(A)** Autoantibodies targeting intracellular neuronal antigens (Ag, blue asterisks), while the antigen is also expressed by the tumor. Cytotoxic T cells surround the neuron and cause an indentation with the help of granzyme B and perforin mechanisms that leads to cell degeneration. **(B)** Autoantibodies targeting extracellular neuronal antigens such as the cell surface proteins *N*-methyl-d-aspartate receptor (NMDAR) or α-amino-3-hydroxy-5-methyl-4-isoxazolepropionic acid receptor (AMPAR), which show a direct interaction between antigen and autoantibody leading to internalization of the receptors and to a loss of receptor density on the cell surface. It is known that these autoantibodies have a direct pathogenic effect on the targeting antigen. Copyright: J. Dalmau, C. Geis, and F. Graus, "Autoantibodies to Synaptic Receptors and Neuronal Cell Surface Proteins in Autoimmune Diseases of the Central Nervous System," *Physiol. Rev.*, vol. 97, no. 2, pp. 839–887, Apr. 2017

The first intracellular antibody was reported in 1983 and characterized as anti-Purkinje cell antibody type 1 (PCA-1) ("anti-Yo") in patients with paraneoplastic cerebellar degeneration [16], followed by the detection of antineuronal nuclear antibodies type 1 (ANNA1) ("anti-Hu") autoantibodies in 1985 in patients with paraneoplastic sensory neuronopathy [17][18]. Anti-Hu autoantibodies are described as the most frequent intracellular autoantibodies [19]. Since then, several autoantibodies targeting neuronal and glial proteins have been discovered. A new era of antibody-associated AIE was opened with the discovery of autoantibodies directed against surface antigens that requires modified detection methods to preserve the three-dimensional structure of the targeted antigen. With these novel diagnostic tools, the prevalence of antibody-associated AIE is even approaching that of infectious encephalitis [20].

Symptoms can range from psychiatric anomalies and memory loss to epileptic seizures and movement disorders, depending on the targeted autoantibody [21][22][23]. These symptoms often make antibody-associated AIE clinically apparent, leading to their early identification and treatment, which can ultimately improve patient outcome. Due to the frequent association with paraneoplastic events, a diagnosis may aid finding an associated underlying tumor [7]. Nevertheless, symptoms may overlap with other disorders and should be considered in a differential diagnosis, including encephalopathies such as Hashimoto's and other steroid-responsive encephalopathies, neuromyelitis optica spectrum disorders (NMOSD), Creutzfeldt-Jakob disease (CJD) and other rapidly evolving dementias, human immunodeficiency virus (HIV) infection, or human herpes virus-6-associated encephalitis [24][25].

Triggers of neuronal cell surface/synaptic antibody-associated AIE vary with respect to the target proteins, with viral infections or tumors often being discussed as possible triggers.

Antibody-associated AIE after viral infections occurs rarely and is mainly described in patients with herpes simplex virus encephalitis (HSE), who have developed autoantibodies against neuronal cell surface proteins, the most common example being the N-methyl-D-aspartate receptor (NMDAR) associated with anti-NMDAR-encephalitis [26][27]. As illustrated in **Figure 3**, the virus causes inflammation within the brain, leading to necrosis of brain tissue. It is discussed that necrotic tissue may release the later targeted antigen and elicit an immune response by activating B cells, which reach the brain through the bloodstream. After restimulation, differentiation and maturation of B

cells into plasma cells, the autoantibodies that cause an antibody-associated AIE may be released.

Antibody-associated AIE triggered by tumors has commonly a better prognosis compared to PNS associated with intracellular antibodies, due to the reversibility of the neurological dysfunction. The paraneoplastic trigger mechanism is illustrated in **Figure 3** by the example of anti-NMDAR encephalitis associated with an ovarian teratoma [7].
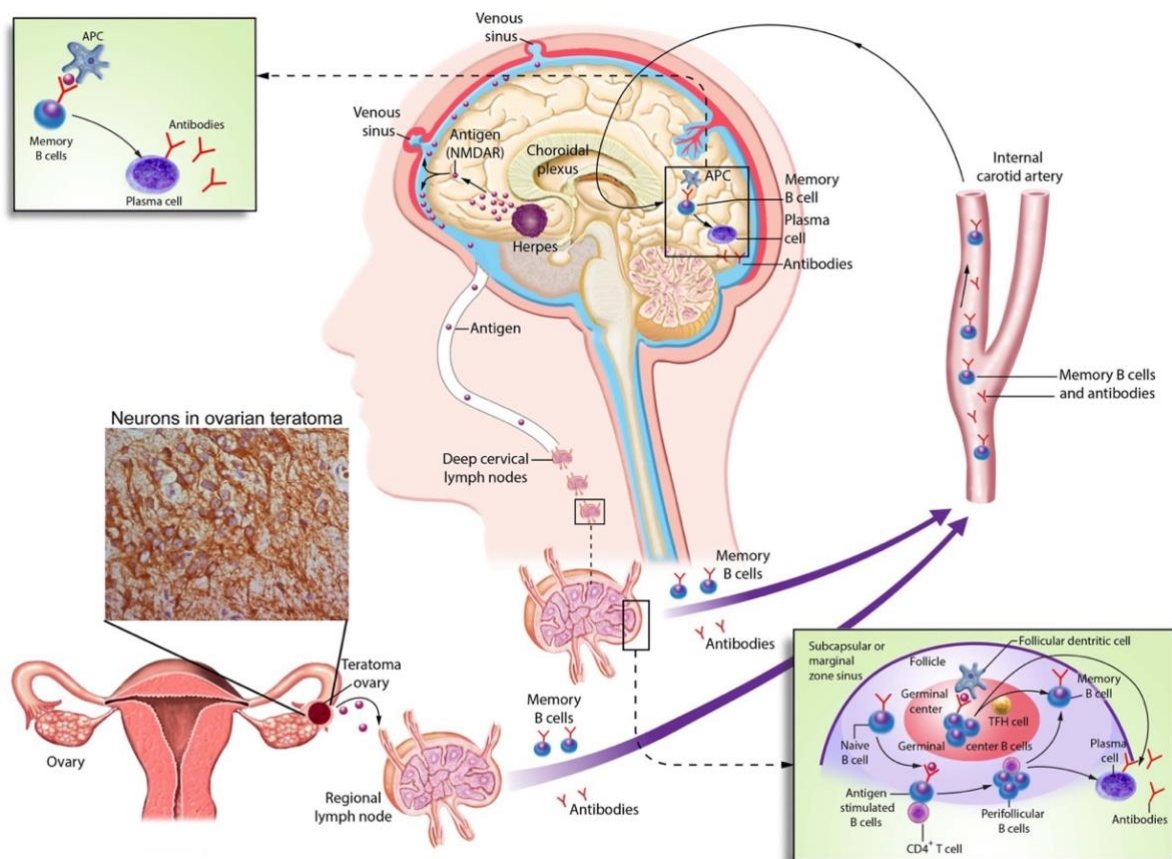
Figure 3: A model of paraneoplastic (usually ovarian teratoma) and viral (herpes simplex virus) triggers using the example of anti-NMDAR encephalitis. The ovarian teratoma contains neurons expressing NMDAR, which are released from the tissue through necrotic changes, reach a regional lymph node, and trigger naive B cells to differentiate into memory B cells and plasma cells. Memory B cells pass the BBB and differentiate into plasma cells by restimulation, which trigger an immune response. HSE triggers the immune system through inflammation, necrosis, and neurodegeneration, which could release the NMDAR antigen that reaches a deep cervical lymph node and cause the autoreactive immune response similar to the paraneoplastic trigger. Copyright: J. Dalmau, C. Geis, and F. Graus, "Autoantibodies to Synaptic Receptors and Neuronal Cell Surface Proteins in Autoimmune Diseases of the Central Nervous System," *Physiol. Rev.*, vol. 97, no. 2, pp. 839–887, Apr. 2017. BBB= blood-brain-barrier, HSE= herpes simplex virus encephalitis, NMDAR= N-methyl-D-aspartate receptor

As briefly mentioned earlier in this section, some intracellular antibodies are associated with tumors in over 90% of cases (high-risk antibodies), and the location of the tumor may correlate with the specific antigen [11][28]. It is discussed that tumor cells aberrantly express neuronal proteins, which causes a failure of self-tolerance and triggers an autoreactive immune response. Antigen presenting cells (APCs) are described to take up remnants of apoptotic cancer cells, process them, and present their protein to naive T and B cells in the regional lymph node, causing an anti-cancer immune response and at the same time an autoimmune reaction against the onconeural protein in the brain, which is illustrated in **Figure 2A** [7][13].

Intracellular autoantibodies may occur with or without cancer and can be directed against neuronal antigens such as ANNA-1 ("Hu"), PCA-1 ("Yo"), ANNA-2 ("Ri"), CV2, Ma1/2, PCA-2, amphiphysin, and GAD65 or glial antigens such as glial fibrillary acidic protein (GFAP) [11].

In this master thesis the focus is on the intracellular protein GFAP, the major intermediate filament in mature astrocytes, which will be described in more detail in the next sections [29].

1.2 Physiology of astrocytes

Astrocytes are the most abundant representative glia in the mammalian brain. They occur in the CNS including the brain and the spinal cord. Astrocytes are divided into four different phenotypes, depending on their location: fibrous, interlaminar, protoplasmic, and varicose projection astroglia, which are located in various layers of the cortex and in the white matter [30][31]. The primary function of astrocytes is not 100% clear, but the main roles include maintaining a normal CNS physiology, synaptogenesis, metabolic support, clearance of neurotransmitters, BBB development and maintenance, and ionic homeostasis. Further functions have yet to be described [26]–[30].

Astrocytes differ morphologically and anatomically, while they all express GFAP – a trait found in mammalian brains [31].

1.2.1 Function of GFAP

The intracellular protein GFAP is the major intermediate filament in mature astrocytes, and is part of their cytoskeleton and scaffold, and therefore essential for maintaining the morphology of astrocytes. Furthermore, it shows functions in cell communication and BBB formation [29]. Additionally, GFAP is used as a marker for mature astrocytes [31].

After astrocyte development and specification, the differentiation process is specified by the induction of GFAP. The regulation of GFAP is maintained through key pathways, such as JAK/STAT and CNTF/LIF/CT-1 cytokine signaling by gp130, while more pathways are involved in the regulation of its expression. Moreover, not only the intracellular pathways are important, but also the extracellular neurohumoral environment plays a major role in regulating the intermediate filament GFAP. Abnormal expression of GFAP can play a role in CNS diseases or trauma, and correlates with the severity of the injury, thus resulting in reactive astrocytes. This explains, why GFAP plays an important role as a biomarker for such events [35]. The benefit of reactive astrocytes is disputed. It is described that their presence leads to inhibition of axon growth and glial scarring. But on the contrary, its ablation increases neuronal cell loss and local inflammation. Concluding that its function is to protect the injured area, preventing the spread of infectious agents or inflammatory cells [33].

There is also a correlation found between upregulated GFAP levels in astrocytes and neurodegenerative diseases such as Alexander disease, Alzheimer´s disease (AD) or Parkinson´s disease, psychiatric diseases and others [33][35].

However, not only diseases can be generated by astrocyte reactivity, but diseases can also affect astrocytes themselves. This diseases are called astrocytopathies [36].

1.2.2 Astrocytopathies

Neuromyelitis optica (NMO) belongs to the group of Neuromyelitis optica spectrum disorders (NMOSD) [37]. NMO is a syndrome, where IgG autoantibodies are selectively directed against the water channel protein aquaporin 4 (AQP4), which is placed on the end feet of astrocytes [38]. Therefore, it is considered as an autoimmune astrocytopathy and can be distinguished from other demyelinating disorders such as multiple sclerosis. This disorder leads to an extensive astrocyte dysfunction and loss and progresses to neuronal and myelin damage [39].

Another example for an astrocytopathy is called Alexander disease. Alexander disease is a degenerative astrocytopathy, which is caused by a gene mutation of GFAP. This disease leads to white matter degeneration and different degrees of neuronal cell loss [40].

Lastly, a prominent example described in some literature as an astrocytopathy is GFAP astrocytopathy [37]–[39]. This disorder describes an autoimmune meningo-encephalomyelitis, where IgG autoantibodies are directed against the intracellular protein GFAP [44]. In the next sections of this master thesis, the current knowledge of this CNS disorder will be further described.

1.3 GFAP meningo-encephalomyelitis

Anti-GFAP meningo-encephalomyelitis is a relatively novel autoimmune-associated brain disorder, first described in 2016 [41]. In some literature, this disorder is also referred to as an astrocytopathy [41]–[43][45]–[48]. Primarily, an astrocyte-specific immunoglobulin type G (IgG) autoantibody, most prominently detected in patients' CSF, binds to GFAP, a cytosolic protein. Therefore, it belongs to the group of antibody-associated AIE, where autoantibodies are directed against intracellular antigens. Despite other antibody-associated AIE against intracellular antigens (e.g. anti-Hu), patients show good response to corticosteroids and immunotherapy [42]. The origin and trigger of this disorder remains mostly unclear, but an association with neoplasms has been described. It is disputed, whether a viral infection can be a possible trigger of anti-GFAP antibody associated meningo-encephalomyelitis [37]–[39][45].

GFAP-related meningo-encephalitis has been described in dogs prior to the discovery of this disorder in humans and can neuropathologically present as necrotizing meningo-encephalitis (NME), granulomatous meningo-encephalomyelitis (GME), and necrotizing leukoencephalitis (NLE). Although some parallels can be seen between these two disorders, the zoonotic version has a much more fatal outcome [42][49].

1.3.1 Epidemiology and patient demographics

GFAP meningo-encephalomyelitis is described as a rare disorder, although it is probably still under-diagnosed. The median age at disorder onset is described at around 45 years with variations between different studies [41][46][47]. Some studies describe a slight female predominance, particularly in patients with a paraneoplastic (ovarian) teratoma [42][47]. Nevertheless, a recently published pooled analysis found no gender predominance in GFAP meningo-encephalomyelitis patients [46]. The incidence in children is estimated at 10% of cases of GFAP meningo-encephalomyelitis [47].

The prevalence of this autoimmune meningo-encephalomyelitis in Olmsted County, Minnesota has been calculated to be 0.6/100 000 [20]. Ethnic predominance has not been found yet. Generally, epidemiological data of this novel disorder are still limited and heterogeneous, making a valid meta-analysis challenging [42][46][47].

1.3.2 Etiology and Pathogenesis

The data and information regarding etiology and pathogenesis of GFAP meningo-encephalomyelitis is still limited. 22% of patients with GFAP meningo-encephalomyelitis were diagnosed with an underlying tumor, suggesting an association between GFAP meningo-encephalomyelitis and paraneoplastic events [43]. The most prominent example is an ovarian teratoma, found in 75% of patients [47]. Other tumors do occur, but in a broad diversity and rarity. Examples include multiple myeloma, adenocarcinomas in various organs and tissues, and gliomas [42][45][47].

It is debated whether GFAP meningo-encephalomyelitis can be triggered by a viral infection [42]. There are case reports of GFAP meningo-encephalomyelitis being diagnosed after herpes simplex encephalitis (HSE), suggesting that there may be a relationship between HSE and GFAP meningo-encephalomyelitis [50][51]. Another study detected GFAP meningo-encephalomyelitis in a patient weeks after a varicella zoster viral encephalitis [52]. These reports raise the possibility of an association between GFAP meningo-encephalomyelitis and an infection with a viral trigger. In case of NMDAR-Ig encephalitis, herpes simplex virus encephalitis is a well-known but uncommon trigger [26]. The pathogenesis is described in section 1.1.1.

Autoantibodies against anti-GFAP can occur simultaneously with other anti-neuronal autoantibodies. Approximately 40% of GFAP meningo-encephalomyelitis cases harbor concomitant humoral autoantibodies against neuronal structures in CSF or serum of patients. The most common concomitant autoantibodies were against NMDAR, followed by anti AQP4-immunoglobulines. These overlapping syndromes are described in more detail in section 1.3.7 [43][52].

Furthermore, it is described that co-existing autoimmune disorders can play a role in the pathogenesis of GFAP meningo-encephalomyelitis. One study found a correlation of approximately 20% with autoimmune disorders such as autoimmune thyroid disorder, type I diabetes mellitus, and rheumatoid arthritis [43][47].

1.3.3 Clinical findings

GFAP meningo-encephalomyelitis often occurs subacutely or acutely, worsens progressively or worsens in episodes. Clinical manifestations include signs and symptoms of meningo-encephalomyelitis, such as encephalopathy, headache, fever, ataxia, epilepsy, abnormal vision, mental disorder and others [42]. The most common clinical symptoms

are infectious prodromal symptoms. One study found an occurrence of 82% in patients with GFAP meningo-encephalomyelitis [53].

In a study of 102 patients with GFAP meningo-encephalomyelitis, clinical findings showed that 81% of the patients had either one or a combination of meningitis, encephalitis, and/or myelitis. Only 3% of the patients showed all three syndromes together. 42%, and therefore the majority of GFAP positive patients were diagnosed with encephalitis, followed by meningo-encephalitis with 12.5% and myelitis with 10.5%. Encephalomyelitis was described in only 8% of patients [43]. Analysis in one study generally demonstrated that the most common clinical symptom showed a subacute meningo-encephalitis in 85% of cases with a cerebellar dysfunction in 57%. Moreover, the peripheral nervous system and vision also showed involvement in the clinical presentation [53].

1.3.4 Laboratory findings

Anti-GFAP IgG autoantibodies can be detected in serum and/or CSF. Generally, CSF has a higher sensitivity to these autoantibodies than serum. One study showed that 94% of anti-GFAP IgG positive patients had antibodies in CSF, while only 67% showed a seropositivity. Another study showed that all tested anti-GFAP IgG positive patients had autoantibodies detected in CSF [44]. Furthermore, all positive patients (100%) had autoantibodies against the alpha-isotype of GFAP, GFAPα, in CSF and/or serum. 81% of the patients were also sensitive to the epsilon-isotype and only 54% of the patients were positive to the kappa-isotype of GFAP. It is also possible that IgG binds against more than one isotype. The antigen isoform does not correlate with the frequency of cancer detection, or with the frequency of meningo-encephalomyelitis diagnosis [43]. In general, the presence of anti-GFAPα IgG autoantibodies found in patient's CSF and/or serum correlate with GFAP meningo-encephalomyelitis [43][54].

Elevated CSF white blood cell counts (WBC) have been identified in the majority of patients with GFAP meningo-encephalomyelitis [42]. This finding was observed in 88% of patients in one study [43]. The normal range of a WBC is 0-8 x 10^6/L, while the median in anti-GFAP IgG positive patients was 230 x 10^6/L in CSF with a range of 16-1600 x 10^6/L. The elevated white blood cells include monocytes and granulocytes, but most prominently showed a predominant elevation in lymphocytes. Additionally, no signs of an infection were found. Furthermore, most patients showed elevated, sometimes even highly-elevated protein levels in CSF with values over 1000 mg/L. The reference value for

protein in CSF is in the range of 150-450 mg/L. Another abnormality were CSF-exclusive oligoclonal bands reported in 54% of patients in one study [43][46].

1.3.5 Imaging findings

Magnetic resonance imaging (MRI) of the brain and spinal cord of patients with GFAP meningo-encephalomyelitis showed characteristic abnormalities. 70% of patients with GFAP meningo-encephalomyelitis showed MRI brain abnormalities, 65% of whom demonstrated T2 abnormalities, 18% of whom contrast enhancement, and 12% of whom pia meningeal enhancement [46]. Furthermore, lesions were found in the basal ganglia, brainstem, cerebellum, hypothalamus, meninges, medulla, skull, ventricle and spinal cord [42][54]. Characteristic T1 and T2 hyperintensities and gadolinium enhancements are shown in **Figure 4** and **Figure 5.** Strikingly, as illustrated in **Figure 4**, MRI of an anti-GFAP IgG-positive patient showed a characteristic linear radial perivascular post gadolinium pattern in the white matter perpendicular to the ventricles on T1 enhancement. This pathology demonstrates inflammation around small blood vessels indicating a damaged BBB through the leakage of gadolinium [55].
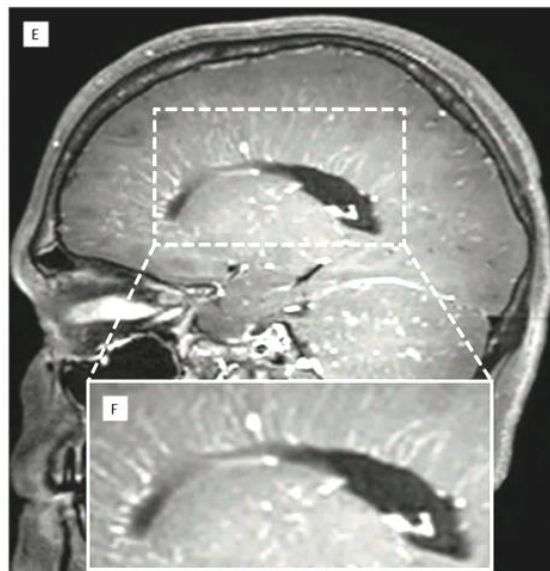
Figure 4: **(E)** Brain MRI (T1, sagittal) showing a periventricular contrast enhancement with a characteristic radial pattern. **(F)** A detailed illustration of this characteristic enhancement. Copyright: B. Fang *et al.*, "Autoimmune Glial Fibrillary Acidic Protein Astrocytopathy: A Novel Meningoencephalomyelitis," *JAMA Neurol.*, vol. 73, no. 11, pp. 1297–1307, Nov. 2016

Additionally, spinal and infratentorial lesions (see **Figure 5**) were found in three anti-GFAP IgG positive patients, with a characteristic appearance of longitudinally extensive T2-

hyperintensities. Overall, MRI abnormalities are more detectable in post gadolinium T1-weighted images [43].

Furthermore, cases with splenic lesions on MRI accompanied by mild encephalitis, especially in children, have been described. The presentation of mild encephalitis with reversible splenial lesion syndrome (MERS) has been mainly documented in anti-GFAP IgG positive patients presenting with post infectious symptoms [56].
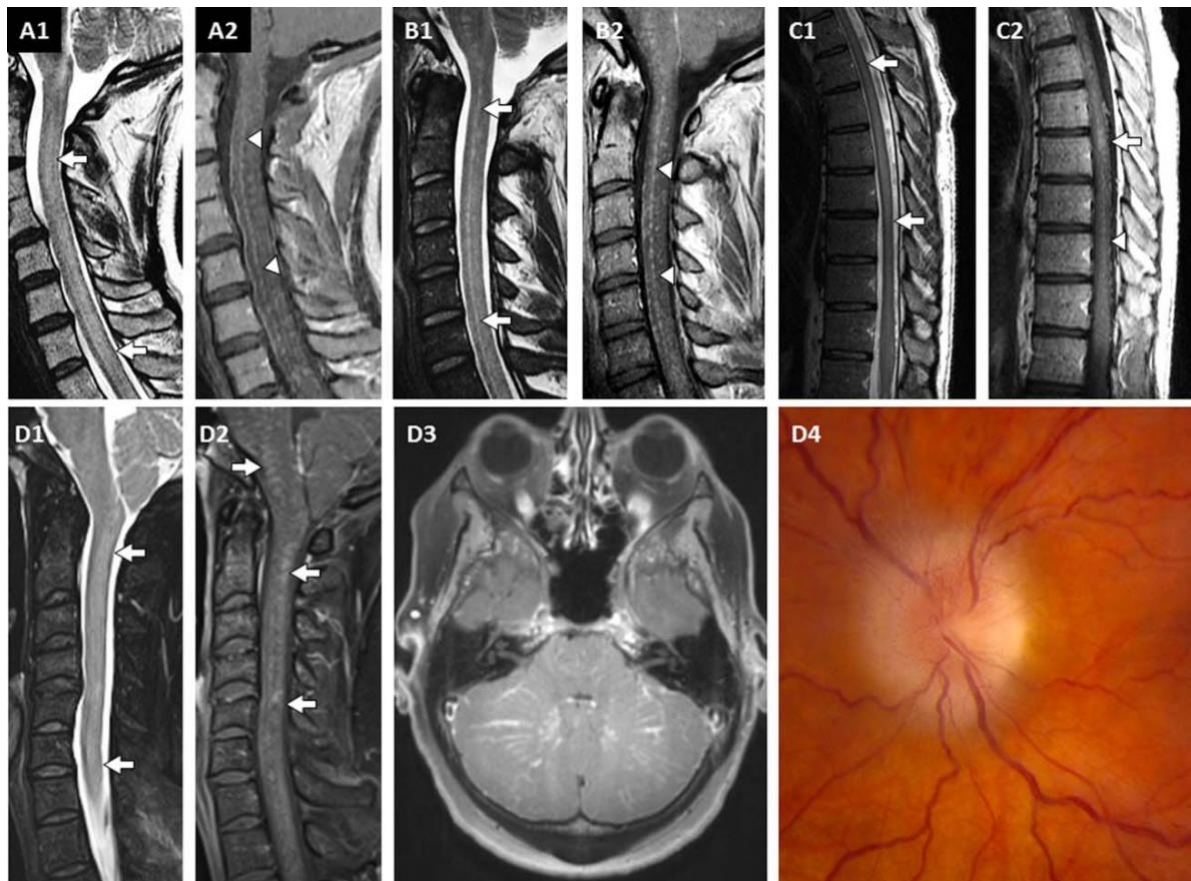
Figure 5: MRI scans of patients with GFAP meningo-encephalomyelitis and their characteristic findings in the spinal cord **(A1-D2),** cerebellum **(D3)**, and a fundoscopy showing a disk edema **(D4)** responsible for blurred vision. Copyright: E. P. Flanagan *et al.*, "Glial fibrillary acidic protein immunoglobulin G as biomarker of autoimmune astrocytopathy: Analysis of 102 patients," *Ann. Neurol.*, vol. 81, no. 2, pp. 298–309, Feb. 2017.

Lastly, a 2-Fluor-2-desoxy-D-glucose Positron-emission-computed tomography (FDG-PET) scan of an anti-GFAP IgG positive patient revealed diffuse inflammation through an increase in FDG uptake [52].

1.3.6 Neuropathological findings

Neuropathological data on GFAP meningo-encephalomyelitis is still limited. Until recently there has been only one published post mortem autopsy report. The case report included

a 70-year-old man with GFAP meningo-encephalomyelitis with a coexisting neuroendocrine tumor and poor response to treatment. Neuropathological findings were mainly unspecific with diffuse inflammation in the brain parenchyma, leptomeninges, and perivascular spaces. Inflammation was predominantly T cell mediated with macrophages and activated microglia. Furthermore, no astrocyte involvement, including GFAP decrease or loss, could be observed, indicating no direct pathogenicity of anti-GFAP IgG against astrocytes [57].

Biopsy reports also remain very limited, however some biopsies showed inflammatory cells surrounding small vessels, while no necrotic changes were detected, and the vessel wall was still intact. Therefore, there is no evidence of vasculitis caused by GFAP meningo-encephalomyelitis in these patients. In the brain, there was extensive infiltration of CD20^{+} B and CD3^{+}/ CD4^{+} T cells around vessels, as well as eosinophilic and disseminated neutrophilic segmented granulocytes. Abundant microglia were also present in neuropathological analysis. Additionally, infiltration of plasma cells was described [42].

In general, immunohistochemical findings suggest that demyelination and astrocyte loss are not associated with GFAP meningo-encephalomyelitis. Moreover, no loss in GFAP or Myelin Oligodendrocyte Glycoprotein (MOG) expression was associated with anti-GFAP IgG autoantibodies [58]. It is discussed that the pathology of GFAP meningo-encephalitis is heterogeneous, while different degrees of severity in AQP4 and GFAP dislocation on astrocytes have been described [42].

That kept in mind, still limited data on local biopsy and autopsy reports cannot reflect the full pathology of GFAP meningo-encephalomyelitis and further studies are important to gain clarity about this disorder [42][43].

1.3.7 Overlapping Autoimmune Syndrome

GFAP meningo-encephalomyelitis may be accompanied by other neuronal or glial antigen targeted autoantibodies. A study by Flanagan et al showed that 40% of anti-GFAP IgG positive patients had concomitant autoantibodies in CSF or serum [43]. Another study by Iorio et al found five out of 22 anti-GFAP IgG positive patients with coexisting neuronal autoantibodies [54]. Moreover, a French cohort study showed an occurrence of 22% GFAP IgG antibody positive patents with coexisting autoantibodies [53]. This suggests that a co-occurrence of GFAP meningo-encephalomyelitis with other neuronal autoantibodies is common. Proven concomitant neuronal/glial autoantibodies are e.g., NMDAR and

AQP4 autoantibodies, and more rarely MOG autoantibodies. One study also found unknown neuronal autoantibodies in three out of thirty anti-GFAP IgG positive patients [59]. These different autoantibodies do not have to occur simultaneously. For example, one patient developed GFAP meningo-encephalomyelitis one year after anti-NMDAR encephalitis. Another example was a patient, who was found to have a positive anti-GFAP IgG titer ten years after being diagnosed with neuromyelitis optica (NMO) [59].

The most common antibody-associated AIE that can coexist with GFAP meningo-encephalomyelitis is anti-NMDAR encephalitis, in which the autoantibodies can be present either simultaneously at onset or sequentially with years in between [59]. As described in section 1.1.1, anti-NMDAR encephalitis can either be triggered through neoplastic events, or less commonly through viruses, the most prominent example being the herpes simplex virus. Anti-NMDAR encephalitis is often accompanied by an underlying tumor, most frequent being an ovarian teratoma [24][60]. Interestingly, an underlying ovarian teratoma can be detected in both GFAP meningo-encephalomyelitis and anti-NMDAR encephalitis [42], [47]. One case report describes a female patient with an underlying ovarian teratoma associated with co-existing GFAP meningo-encephalomyelitis and anti-NMDAR encephalitis [61].

A second overlapping autoimmune syndrome is found in patients with concomitant anti-GFAP and anti-AQP4 autoantibodies. AQP4 belongs to the family of water channel proteins, whose function is based on the regulation of water permeability. AQP4, a membrane-bound protein, is located at the end feet of astrocytes in the central nervous system, primarily including the optic nerve and/or the spinal cord. AQP4 IgG autoantibodies are mainly detected in patient serum [62][63]. It is discussed that, in contrast to GFAP meningo-encephalomyelitis, AQP4 antibodies result in a loss of antigen expression, ultimately leading to a decrease in astrocytes [42]. A case report of a patient with overlapping neuromyelitis optica spectrum disorder (NMOSD) and the presence of anti-AQP4 autoantibodies, as well as anti-GFAP IgG autoantibodies was presented. The patient showed typical clinical symptoms of GFAP meningo-encephalomyelitis, such as ataxia, fever, and headache, but additionally vision loss and hiccups. Brain MRI revealed a characteristic radial enhancement pattern [64]. The mean onset of this overlapping syndrome of GFAP meningo-encephalomyelitis with AQP4 autoantibodies was younger than in patients without overlapping syndrome, which is the only known significant difference found so far [59].

Lastly, a simultaneous overlapping syndrome of GFAP meningo-encephalomyelitis and MOG IgG autoantibodies has rarely been described in the literature. MOG also occurs predominantly in the optic nerve and the spinal cord. Anti-MOG IgG autoantibodies are commonly detected in patients with an inflammatory demyelinating autoimmune disease and are termed MOG-IgG associated disease (MOG-AD) [65][66].

1.3.8 Treatment Response and Prognosis

Although GFAP is an intracellular antigen, studies have shown significant responses to treatment in many cases [46]. Nevertheless, there are some case reports reporting poor response to typical treatment methods [67]. While general treatment guidelines or criteria for GFAP meningo-encephalomyelitis have yet to be established, treatment strategies are comparable to pharmacologic therapy for common antibody-associated AIE [25][68]. Typically, treatment in the acute stage of this disorder involves intravenous immunoglobulin (IVIG), high-dose corticosteroids, preferably methylprednisolone, prednisolone, dexamethasone, or azathioprine, and plasma exchange [52]. Corticosteroids are reported to show less clinical benefit and a greater likelihood of relapse when administered orally rather than intravenously. Another recommended treatment modality is a combination therapy of oral steroids and immunosuppressants, such as rituximab, cyclophosphamide, or mycophenolate mofetil. Combination therapy of oral steroids with the immunosuppressant azathioprine shows little efficacy in terms of relapse prevention [46]. GFAP meningo-encephalomyelitis relapses have been described in case reports. A patient´s relapse after a successful treatment and improved clinical outcome is illustrated on brain MRI in **Figure 6** [43]. A pooled analysis indicated that an overlapping syndrome of GFAP meningo-encephalomyelitis with AQP4 autoantibodies can result in a poorer response to immunotherapy in the acute stage. In addition, more cases of relapses with diagnosed overlapping syndrome, particularly when AQP4 IgG autoantibodies are co-present, have been reported [46].
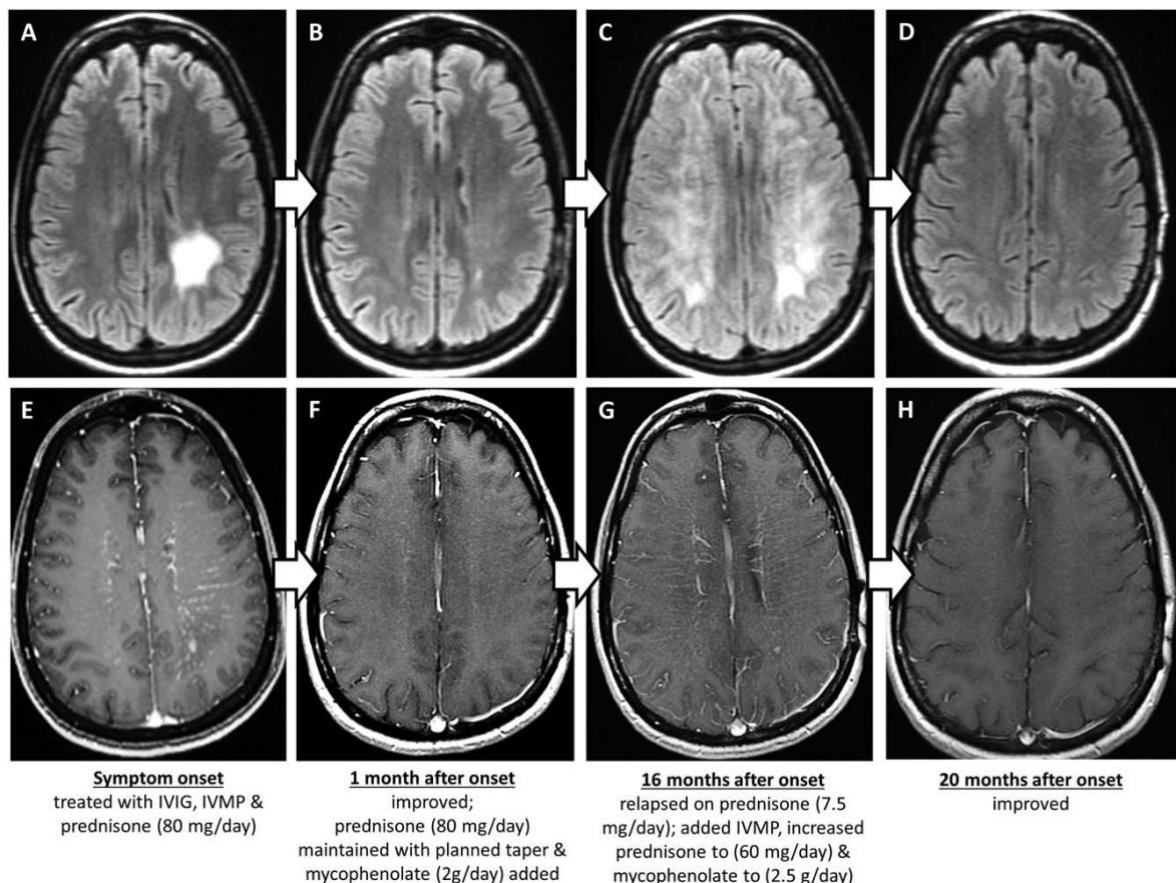
Symptom onset	1 month after onset	16 months after onset	20 months after onset
treated with IVIG, IVMP & prednisone (80 mg/day)	improved; prednisone (80 mg/day) maintained with planned taper & mycophenolate (2g/day) added	relapsed on prednisone (7.5 mg/day); added IVMP, increased prednisone to (60 mg/day) & mycophenolate to (2.5 g/day)	improved

Figure 6: Development of brain MRI findings in patients with relapsing GFAP autoimmune meningo-encephalitis. **(A-D)** demonstrates axial fluid inversion recovery images. **(E-H)** illustrates axial T1 post gadolinium images. Hyperintensities are demonstrated in **(A, E)** at symptom onset. **(B, F)** shows remission one month after treatment. **(C, G)** illustrates a relapse 16 months after onset with characteristic enhancement patterns. Treatment improved MRI hyperintensities illustrated in **(D, H)**. Copyright: E. P. Flanagan *et al.*, "Glial fibrillary acidic protein immunoglobulin G as biomarker of autoimmune astrocytopathy: Analysis of 102 patients," *Ann. Neurol.*, vol. 81, no. 2, pp. 298–309, Feb. 2017. IVIG= intravenous immunoglobulin, IVMP= intravenous methylprednisolone.

1.3.9 Detection methods

Antigen identification and characterization of GFAP was first performed on isolated rat spinal cord proteins probed by Western blot binding with patients' IgG. It revealed an immunoreactive band at about 50kDa between the antibodies and the spinal cord proteins. Immunostaining of mouse tissue of the periventricular region was then performed with the IgG transblotted from this immunoreactive band. IgG also binds the cytoplasm of a glioblastoma multiforme xenograft cell line, similar to GFAP reactive control antibodies. Mass spectrometry of two patients' autoantibody's antigen showed sequences of the GFAP isoforms. In a two-dimensional electrophoretic gel, patients IgG

bound to various polypeptides of GFAP. All IgG were also found to be at least GFAPα reactive using a cell-based assay (CBA) of transfected HEK293 cells [41].

Not only GFAP is localized in astrocytes, but also AQP4, a membrane protein, which is expressed on the endfeet of astrocytes. Detection methods for antibodies directed to AQP4 include tissue-based assay (TBA), CBA, immunoblotting, flow cytometry, and immunoprecipitation. Because of the intracellular localization of GFAP, detection methods for this disorder are limited. Well-known and validated methods include CBA, immunofluorescence assay (IFA), and Western blot. Mouse and rat brain tissue are recommended substrates for TBA. Rat brain tissue shows sensitivity to anti-GFAP IgG autoantibodies, but different subtypes of this protein cannot be distinguished. Moreover, other proteins expressed in astrocytes may confound a positive result for GFAP IgG autoantibodies [42].

Generally, the recommended and mainly used anti-GFAP IgG autoantibody detection methods are IFA and CBA. Cryosections (4 µm) of adult mouse brain tissue were used for IFA. For CBA, a HEK293 cell line transfected with a plasmid encoding a single GFAP transcript variant, preferably using the alpha subtype of the antigen, including a green fluorescent protein (GFP)-tag is recommended for CBA. In one study, the transfected cells grew on poly-D-lysine coated slides, fixed with 4% paraformaldehyde, and permeabilized with 0.2% Triton X-100. The fixed cells were incubated with normal goat serum to prevent non-specific IgG binding, and then exposed to either patient serum diluted 1:200 or CSF diluted 1:4. The cells were then incubated with a secondary antibody and mounted [43].

Coexisting or other neural antibodies show similarities in the detection methods, but different variants in the procedure [69].

2 Aim

The aim of this master thesis project was to search for autopsy cases with GFAP meningo-encephalomyelitis that may contribute to elucidate its pathogenesis, identify novel neuropathological patterns, and find possible triggers. Therefore, patients with an available autopsy and CSF, plasma and/or serum acquired from the Neurobiobank were screened for anti-GFAPα IgG autoantibodies via a fixed CBA. The approach is to find an incidental finding of this disorder in patients due to the heterogenous clinical manifestations of GFAP meningo-encephalomyelitis. In addition, we investigated whether the tissue-based assay optimized for the detection of anti-neuronal surface antibodies (anti-neuronal TBA) is useful to screen for anti-GFAPα IgG autoantibodies.

3 Materials and Methods

3.1 Reagents

All reagents and antibodies used are listed in **Table 1**, **Table 2, Table 3,** and **Table 4**. Laboratory equipment is listed in **Table 5**.

Table 1: Reagents

Product	Company	Location	Product number
2-Methylbutane	Honeywell	Muskegon, USA	12191502
3,3'-Diaminobenzidine /Liquid DAB Plus (DAB)	Dako/Agilent	Santa Clara, USA	K3468
4% Paraformaldehyde (PFA)	Alfa Aesar	Massachusetts, USA	J61899
4´,6-Diamidino-2-phenylindole (DAPI)	Invitrogen	Carlsbad, USA	D1306
70% ethanol	provided by "Vienna General Hospital" AKH hospital pharmacy	Vienna, Austria	F12A3717A7R
Antibody (AB)-Diluent	Dako/Agilent	Santa Clara, USA	K8006
Ampicillin	Sigma-Aldrich	St.Louis, USA	A-9518
Aqua-Poly/Mount	PolySciences	Warrington, USA	18606-20
Bovine serum albumin (BSA)	Sigma-Aldrich	St.Louis, USA	A9647
DMEM/F-12	Gibco, Thermo Fisher Scientific	Waltham, USA	31331-028
Dulbecco´s modified Eagle´s medium (DMEM)	Sigma-Aldrich	St.Louis, USA	D6429
Dulbecco´s Phosphate Buffered Saline (DPBS)	Gibco, Thermo Fisher Scientific	Waltham, USA	14190-094
E.coli DH5α	Invitrogen	Carlsbad, USA	11319019
Fetal bovine serum (FBS)	Gibco, Thermo Fisher Scientific	Waltham, USA	10270-098
Glycerol	Honeywell	Muskegon, USA	G7757
HEK293T cells	kindly provided by the institute		
Hydrogen peroxide	Millipore	Massachusetts, USA	K48743809
Isopropanol	Emsure	Darmstadt	K51877934942
L-glutamine	Gibco, Thermo Fisher Scientific	Waltham, USA	25030-024
Lipofectamine 2000	Gibco, Thermo Fisher Scientific	Waltham, USA	11058-021

Liquid nitrogen	Messer SE & Co. KGaA	Bad Soden am Taunus, Germany	0092*
Luria Broth Base (LB)	Invitrogen	Carlsbad, USA	12795027
MEM Non-essential Amino Acid Solution	Sigma-Aldrich	St.Louis, USA	M7145
n-Butyl-acetate	Supelco	Pennsylvania	K52982952
Normal donkey serum	Millipore	Massachusetts, USA	566460
Opti-MEM	Gibco, Thermo Fisher Scientific	Waltham, USA	11058-021
Penicillin-streptomycin (Pen-Strep)	Sigma-Aldrich	St.Louis, USA	P4333
Phosphate-buffered saline (PBS)	Morphisto	Frankfurt am Main, Germany	11232
Poly D-lysine hydrobromide	Sigma-Aldrich	St.Louis, USA	P7886
Qiagen HiSpeed Plasmid Maxi Kit	Qiagen	Hilden, Germany	12663
Sodium hypochlorite	Roth	Karlsruhe, Germany	9062.1
Sterile Aqua dist.	B. Braun	Hessen, Germany	0082423E
Streptavidin-horseradish peroxidase (HRP)	Dako/Agilent	Santa Clara, USA	K0675
Sucrose	Merck KgaA	Darmstadt, Germany	1.076.511.000
Tissue-Tek O.C.T (optimal cutting temperature compound)	Scigen Scientific	Gardena, USA	4586
Triton X-100	Sigma-Aldrich	St.Louis, USA	T8787
Trypsin-EDTA solution	Sigma-Aldrich	St.Louis, USA	T4049

Table 2: Qiagen HiSpeed Plasmid Purification reagents and composition

Buffer	Composition	Storage
Buffer P1 (resuspension buffer)	50 mM Tris-Cl, pH 8.0; 10 mM EDTA; 100 µg/ml RNase A	2-8°C, after addition of RNase A
Buffer P2 (lysis buffer)	200 mM NaOH, 1% SDS (w/v)	15-25°C
Buffer P3 (neutralization buffer)	3.0 M potassium acetate, pH 5.5	15-25°C or 2-8°C
Buffer QBT (equilibration buffer)	750 mM NaCl; 50 mM MOPS, pH 7.0; 15% isopropanol (v/v); 0.15% Triton X-100 (v/v)	15-25°C
Buffer QC (wash buffer)	1.0 M NaCl; 50 mM MOPS, pH 7.0; 15% isopropanol (v/v)	15-25°C
Buffer QF (elution	1.25 M NaCl; 50 mM Tris-Cl, pH 8.5; 15%	15-25°C

buffer)	isopropanol (v/v)	
TE	10 mM Tris-Cl, pH 8.0; 1 mM EDTA	15-25°C

Table 3: Primary antibody

Antibody	Company	Location	Product number	Host	Application	Dilution
anti-GFAP	Dako	Santa Clara, USA	Z0334	Rabbit	CBA	1:3000

Table 4: Secondary antibodies

Antibody	Company	Location	Product number	Species	Application	Dilution
Alexa Fluor® 594 AffiniPure goat anti-human IgG	Gibco, Thermo Fisher Scientific	Waltham, USA	A-11014	Human	CBA	1:750
Cy3 goat anti-rabbit	Jackson Immuno Research	Pennsylvania, USA	111-165-144	Rabbit	CBA	1:750
biotinylated donkey anti-human IgG	Jackson Immuno Research	Pennsylvania, USA	709-065-149	Human	CBA	1:2000

Table 5: Lab equipment

Lab equipment	Company
Autostainer Link 48 system	Dako/Agilent
Bacterial incubator	Ecotron, Infors-HT
Centrifuge	Rotina 380R
Fluorescence microscope	Olympus BX63
Humidified incubator	Gibco, Thermo Fisher Scientific
Inverse light microscope	Olympus
Laminar flow hood	HERAsafe
Microm CTM glass coverslipper	Gibco, Thermo Fisher Scientific
Nanodrop spectrophotometer	Gibco, Thermo Fisher Scientific
Neubauer counting chamber	Optik Labor
Rocking platform	Gesellschaft für Labortechnik mbH (GFL)
Light microscope	Nikon Eclipse E400

3.2   Patient information and inclusion criteria

This master thesis included plasma, serum and/or cerebrospinal fluid (CSF) samples from patients that were sent for diagnostic purposes and routinely tested for anti-neuronal surface and/or anti-glial autoantibodies, Creutzfeldt-Jakob disease (CJD) via 14-3-3 protein diagnostic, Alzheimer disease (AD) (determination of β-amyloid and tau concentrations), anti-ganglioside antibodies, and enzyme diagnostics. These samples were then retrospectively selected and acquired from the "Neurobiobank" from the Division of Neuropathology and Neurochemistry (NPC), Department of Neurology, Medical University of Vienna based on two inclusion criteria: (1) patient serum and/or CSF was available for anti-GFAPα screening and (2) the patient's brain autopsy was available for immunohistochemical analysis. This information was accessed via "KINNet", an internal patient database provided by the NPC. 603 patients met the inclusion criteria of which 153 patients had to be excluded due to insufficient or unavailable sample material, so that a total of 450 patients remained for the anti-GFAPα screening.

This study was approved by the ethical committee of the Medical University of Vienna (EK. No. 1123/2015).

3.3   Plasmid preparation

3.3.1   Plasmid transformation and amplification

The plasmid GFAP homo sapiens transcript variant 1 (RG 204548, pCMV6-AC-GFAP-α-GFP), that was used for the transfection of human embryonic kidney cells (HEK293T) as described in section 3.4.3 was amplified with the competent bacteria strain Escherichia coli D5Hα (E. coli) (11319019, Invitrogen; Carlsbad, USA). The E. coli cells were already transformed with the GFAPα plasmid by PhD student Verena Endmayr, MSc using the heat shock method and stored as a glycerol stock at -80°C. In case of a defrost, a reserve glycerol stock was stored in another freezer. The manufacture of a glycerol stock is described later in this section.

For the Luria Broth Base (LB)-Medium, 12.5 g of LB (12795027, Invitrogen; Carlsbad, USA) were dissolved in 500 ml Aqua dist. Then, the LB-Medium and a 1000 ml Erlenmeyer flask were autoclaved for 20 minutes (min) at 121°C. The following steps were executed near a Bunsen burner to ensure an aseptic working environment. Waste was disposed in the black barrel.

For plasmid amplification, the autoclaved flask was filled with 250 ml LB-Medium. Additionally, functioning as a zero control, three ml LB-Medium were filled in a falcon tube, whereby the solution should remain transparent and not turn into a cloudy suspension. A cloudy suspension would indicate bacterial growth and therefore contamination. Since the plasmid contained an ampicillin resistance gene, the antibiotic ampicillin (A-9518, Sigma Aldrich; St. Louis, USA) was used to ensure selection of the right strain of bacteria. Due to photosensitivity of the antibiotic, the concentrated solution had to be protected from any light source. The ampicillin concentration in the LB-medium was adjusted to 100 µg/ml. The usage of beta lactam in the zero control was optional.

For the inoculation, the deep-frozen E. coli glycerol stock was scraped off twice with a sterile 1000 µl tip, covering a ground of three to five mm^3, and diluted in the previously prepared LB-Medium. If there was only a small amount of glycerol stock left, a new one had to be made the following day.

The flask was closed, and the bacterial suspension was incubated overnight for 16 to 21 hours in a bacterial incubator (Ecotron, Infors-HT) at 37°C, shaking at 240 rounds per minute (rpm), resulting in a cloudy suspension. On the next day, the cloudy suspension was decanted into five 50 ml falcon tubes.

As mentioned earlier, if a new glycerol stock was required, three ml of bacterial suspension was removed from the flask, which had been incubated overnight, and pipetted into a sterile tube. Two nunc tubes were labelled with the name of the plasmid, tag, stock, clone, antibiotic resistance, and date of manufacture. Each tube containing the bacterial suspension was slowly and thoroughly resuspended with 530 µl of autoclaved glycerol (G7757, Honeywell; Muskegon, USA) until no more streaks were visible in the suspension. Then, the suspension was divided into the two labelled nunc tubes and stored at -80°C. The storage is analogous to the glycerol stocks mentioned above in 3.3.1. The decanted bacterial suspension was centrifuged with the Rotina 380R centrifuge at 4°C for 10 min at 4400 rpm, leaving a bacterial pellet on the bottom. For decontamination, the supernatant was poured back into the Erlenmeyer flask, filled with 25 ml sodium hypochlorite (9062.1, Roth; Karlsruhe, Germany) and incubated overnight for disposal purposes. The bacterial pellet was then used for the plasmid purification (Maxiprep).

3.3.2 Plasmid purification

Plasmid purification was performed according to the Qiagen HiSpeed Plasmid Maxi Kit`s (12663, Qiagen; Hilden, Germany) protocol. The reagents used were included in the kit and their composition is listed in **Table 2**.

Bacterial lysis

One of the five 50 ml falcons, which contained a bacterial pellet, was resuspended with 10 ml resuspension buffer P1. This suspension was then transferred to the second falcon containing another bacterial pellet and was again well resuspended. This process was continued until all bacterial pellets were united in one falcon. Next, 10 ml of lysis buffer P2 was added, and the falcon was inverted eight to ten times, causing a chemical reaction that colored the suspension blue. The solution was incubated for 5 min. During the incubation period, the QIAfilter Cartridge was prepared by screwing the cap onto the outlet nozzle of the Cartridge, labeling it thoroughly, and placing the Cartridge on the rack. After incubation, 10 ml of prechilled neutralization buffer P3 were added and again inverted eight to ten times. The solution turned transparent showing white cell debris. The lysate containing the plasmid was then poured into the barrel of the prepared QIAfilter Cartridge and incubated at room temperature (RT) for 10 min. During the incubation period, the HiSpeed Maxi column was equilibrated with 10 ml of QBT equilibration buffer by dripping it through the column, until the column was empty. After ten min of incubation, the cap was removed from the QIAfilter Cartridge outlet nozzle and the cell lysate containing the plasmid (without cell debris) was transferred into the equilibrated HiSpeed Maxi column using a QIAfilter plunger. The plasmid solution dripped through the column by gravity flow, allowing the cleared lysate to enter the resin. The resin was rinsed with 60 ml QC washing buffer and afterwards the plasmid was eluted with 15 ml QF elution buffer. The plasmid eluate was collected in a 50 ml falcon by gravity flow.

Precipitation

Precipitation of DNA was performed by adding 10.5 ml isopropanol (K51877934942, Emsure; Darmstadt, Germany) to the eluted DNA in the 50 ml falcon tube. The solution was vortexed and incubated for five min at RT. During the incubation period, the next step for precipitation was prepared. The plunger of a 30 ml syringe was removed and a labelled QIAprecipitator Module was attached onto the outlet nozzle. The

eluate/isopropanol mixture was transferred into the syringe and extruded into the QIAprecipitator Module. Afterwards, 2 ml of 70% pure ethanol was filled into the syringe, which replaced the isopropanol in the Module. Finally, the QIAprecipitator was dried by extruding air ten times into the QIAprecipitator Module.

Elution

After the syringe plunger was removed, the dried QIAprecipitator Module was plugged on a 5 ml syringe. A 1.5 ml sterile Eppendorf collection tube was thoroughly labelled, including plasmid, tag, date, and plasmid concentration, which was determined with the use of a Nanodrop spectrophotometer (Gibco, Thermo Fisher Scientific), as described in section 3.3.3. 1 ml TE buffer was pipetted into the syringe and with the use of a plunger the DNA was eluted into the collection tube. The QIAprecipitator Module was unplugged, the plunger removed, and the QIAprecipitator Module plugged in again. To ensure a high DNA concentration, the eluate was filled again into the 5 ml syringe and eluted for a second time into the same collection tube. The eluted DNA was stored at 4°C until Nanodrop measurement. The long-term storage of the plasmid was at -80°C.

3.3.3   Measurement of DNA concentration – Nanodrop spectrophotometer

After plasmid preparation, the DNA concentration was determined with a Nanodrop spectrophotometer at a wavelength of 260 nm. A total of 2 µl volume of the eluted DNA were required for the measurement. TE buffer was used as a blank value. The DNA measurement was carried out in triplicates, of which the mean value was then determined.

3.4 Anti-GFAPα cell-based assay

3.4.1 Maintenance of HEK293T cells

The HEK293T cell line, also known as human embryonic kidney cells, was used for anti-GFAPα cell-based assays. The growth of the cells was ensured in a humidified incubator (Gibco, Thermo Fisher Scientific,) at 37°C in 5% CO_2 atmosphere. The cell cultivation was performed under sterile conditions in a laminar flow hood (HERAsafe).

HEK293T cells were cultured in a 100 mm Petri dish (p100) with cell growth medium, where Dulbecco´s modified Eagle´s medium (DMEM) − high glucose (D6429, Sigma Aldrich; St. Louis, USA) was mixed 1+1 with DMEM/F-12 (1X) +GlutaMAX^{TM}−I − Dulbecco´s Modified Eagle Medium F-12 Nutrient Mixture (25030-024, Gibco, Thermo Fisher Scientific; Waltham, USA) and supplemented with 10% fetal bovine serum (FBS) (10270-098, Gibco, Thermo Fisher Scientific; Waltham, USA), 2% L-glutamine (25030-024, Gibco, Thermo Fisher Scientific; Waltham, USA), 1% penicillin-streptomycin (Pen-Strep) (P4333, Sigma Aldrich; St. Louis, USA), and 2% MEM Non-essential Amino Acid Solution (100x) (M7145, Sigma-Aldrich; St. Louis, USA).

To maintain the HEK293T cell line, the cells were split twice a week at 70-80% confluency, which was determined with an inverse light microscope (Olympus). Briefly, the cell growth medium was removed and the Petri dish was rinsed twice with 10 ml (1x)-Dulbecco´s Phosphate Buffered Saline (DPBS) (14190-094, Gibco; Waltham, USA) to remove any remaining FBS, that may reduce the trypsin activity. Afterwards, the cells were trypsinized with 2 ml Trypsin-EDTA (T4049, Sigma Aldrich; St. Louis, USA) at 37°C in 5% CO_2 for 2 to 3 min in the humidified incubator. The cells were then resuspended with 6 ml cell growth medium, to stop the trypsinization. The cell suspension was transferred to a 15 ml falcon and centrifuged for three min at 3,200 rpm leaving a cell pellet at the bottom. After centrifugation, the supernatant was decanted and the remaining cell pellet was resuspended with fresh cell growth medium. The number of cells were manually counted using a Neubauer cell counting chamber (Optik Labor, Neubauer improved). Depending on the desired cell density, an appropriate seeding density of cells was seeded onto a p100 Petri dish and suspended with 15 ml fresh cell growth medium. The cells were cultured in the humidified incubator until further cell splitting was necessary.

For anti-GFAPα cell-based assays, cells were seeded in 60 mm Petri dishes (p60) and suspended with 5 ml fresh cell growth medium at appropriate cell densities. Each dish

contained Poly D-lysine hydro bromide (PDL, 10 mg/100 ml) (P7886, Sigma Aldrich; St. Louis, USA) coated glass cover slips as described in section 3.4.2. The different cell densities (time from seeding until transfection) are illustrated in **Figure 7**, and were as follows: (1) seeding density of 0.15 million (M) for a time period of three days until transfection **(Figure 7A, B)**; (2) 0.35M for a time period of two days (**Figure 7C, D**); (3) 0.95M for a time period of one day (**Figure 7E, F**).The different cell densities and time periods from seeding to transfection suggest better confluency and fewer apoptotic cells in 0.15M and 0.35M, than in 0.95M.
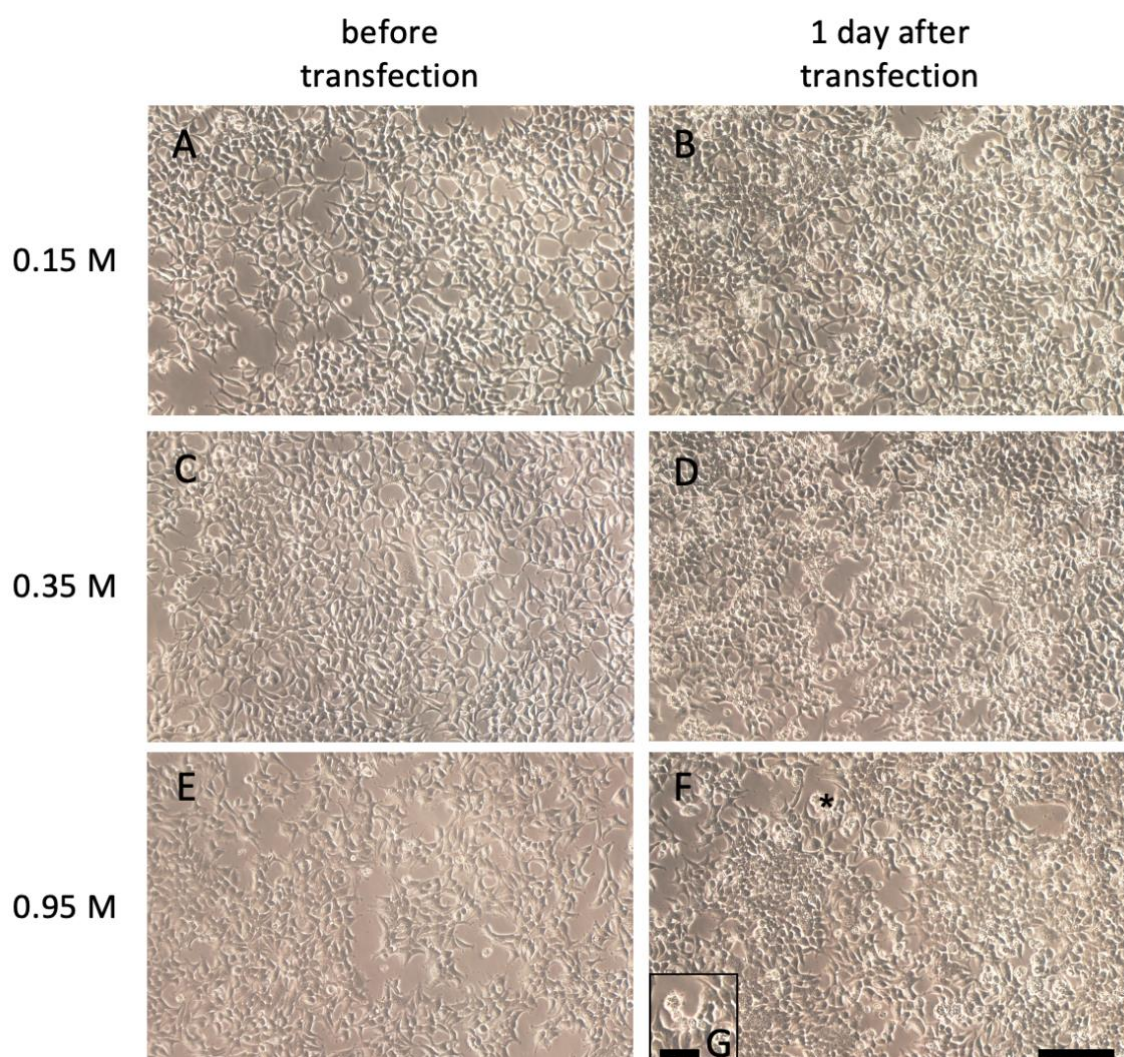
Figure 7: HEK293T in different seeding densities and days of growth, showing different rates of confluency and apoptotic cells. **(A, C, E)** HEK293T cells on the day of transfection. **(A)** Three days after the cells were seeded at a density of 0.15 million (M) on a Petri dish. The confluency is 90% and apoptotic cells rarely occur. **(C)** The cells were seeded 0.35M with two days of growth until transfection. The confluency and occurrence of apoptotic cells are comparable to **(A)**. **(E)** HEK293T cells were seeded 0.95M with a one-day growth period until transfection. The confluency is 80% and therefore lower than in **(A)** and **(C)**. The number of apoptotic cells is comparable to **(A)** and **(C)**. **(B, D, F)** HEK293T cells one day after transfection. In general, more apoptotic cells are visible and confluency has

increased. **(B)** The cell layer is homogeneous and shows a confluency of 95%. **(D)** The cells and confluency are comparable to **(B)**. **(F)** The confluency with 85% is lower than in **(B)** and **(D)**. Additionally, the presence of apoptotic cells is higher. Asterisk: round apoptotic cells detached from cell layer **(G)**. Scale bar **(A-F)**: 300 µm. **(G)**: 100 µm. M= million

3.4.2 Coating of glass coverslips

The following protocol was performed under sterile conditions in a laminar flow hood. To prevent cell detachment while performing CBA, glass coverslips (Ø 12 mm, Costar; Cambridge, MA, USA) were coated with ready-to-use (r.t.u.) PDL. For the PDL stock solution, 5 mg PDL was dissolved in 2 ml sterile distilled water (Aqua dist.) (0082423E, Fa. B. Braun: Hessen, Germany). Then, the 2 ml stock solution was diluted with 48 ml sterile Aqua dist. to obtain the r.t.u. PDL-solution.

Each well of a 24-well-plate was filled with 500 µl r.t.u. PDL solution. Autoclaved glass coverslips were placed in each well. The coverslips were incubated with PDL for at least two hours in the humidified incubator at 37°C and 5% CO_2.

Afterwards, coverslips were washed with sterile Aqua dist. Therefore, three wells of a six well plate were filled with sterile Aqua dist. Each PDL coated glass cover slip was rinsed three times with Aqua dist. The washed glass cover slip was placed in a p60 Petri dish with the coated side facing upwards. Each dish was filled with a maximum of twelve coverslips. Then, they were disinfected via UV light in a laminar flow hood. The coated and disinfected coverslips were stored in the humidified incubator at 37°C and 5% CO_2, until they were used for the anti-GFAPα cell-based assay. The 24-well plate could be used for coating of glass coverslips for up to two months.

3.4.3 Transfection of HEK293T cells with GFAPα plasmid

HEK293T cells were transfected with 8 µg plasmid DNA per p60 Petri dish using lipofectamine 2000 as a transfection reagent. The plasmid GFAP homo sapiens transcript variant 1 (RG 204548, pCMV6-AC-GFAP-α-GFP) was used for the transfection of HEK293T cells. The following protocol was performed under sterile conditions in a laminar flow hood.

250 µl Opti-MEM–Reduced Serum Medium (11058-021, Gibco; Waltham, USA) was filled in one autoclaved Eppendorf tube. 12 µl lipofectamine 2000 reagent (11058-021, Invitrogen; Waltham, USA) was added to the tube and was vortexed well. In a second

tube, 250 µl Opti-MEM was united with the required amount of GFAPα plasmid. Both tubes were incubated for five min at RT. Then, the Opti-MEM/lipofectamine solution was mixed together with the Opti-MEM/plasmid solution and incubated for 30 min at RT. After incubation, the mixture was slowly pipetted into the p60 Petri dish and was then incubated overnight in the humidified incubator at 37°C and 5% CO_2. On the following day, an intracellular staining was performed on the transfected cells using a fixed CBA.

3.4.4 Intracellular staining – fixed cell-based assay

Since GFAP is an intracellular protein, a fixed indirect immunofluorescent CBA was performed. By fixing and permeabilizing the transfected cells, anti-GFAPα IgG autoantibodies can reach the target antigen by passing through the cell's plasma membrane. As a result, anti-GFAPα IgG autoantibodies can be detected. For each CBA, three controls were used:

1. human positive control: rAb301 (0.15 mg/ml); the recombinant anti-GFAPα Fc-part IgG1 antibody provided by Prof. Klaus Dornmair was used as a positive control for the CBA with GFAPα. This positive control was used for each p60 Petri dish to ensure valid results. The recombinant antibody was diluted 1:1000 in 10% Antibody (AB)-Diluent (K8006, Dako/Agilent; Santa Clara, USA). AB-Diluent was diluted 1:10 in 1xPBS.

2. commercial positive control (Z0334, Dako/Agilent; Santa Clara, USA): a recombinant primary anti-GFAP polyclonal rabbit antibody was used to ensure a correct transfection and translation of GFAPα. The dilution was set at 1:3000 in 10% AB-Diluent.

3. Antinuclear Antibody's (ANA's) control: a patient sample that functioned as a secondary anti-human IgG antibody (AF594) control. When evaluated under a fluorescence microscope, antinuclear antibodies were visible.

Due to the green fluorescent protein (GFP) tag on the GFAPα plasmid, the following protocol was performed in the dark. The staining procedure did not require a sterile environment.

The medium in the p60 Petri dish was removed with a Pasteur pipette. Then, the cells were washed once with 1xPBS, a 1:10 dilution of 10xPBS (11232, Morphisto; Frankfurt am Main, Germany) in Aqua dist. Afterwards, the HEK293T cells were fixed with prechilled 4% paraformaldehyde (PFA) (J61899, Alfa Aesar; Massachusetts, USA) and incubated for 10

min at RT. The cells were then washed three times with 1xPBS, permeabilized using 0.3% Triton X-100 (T8787, Sigma Aldrich; St. Louis, USA) and incubated for five min at RT. The cells were again washed three times with 1xPBS. The fixed and permeabilized cells were incubated in 1% bovine serum albumin (BSA) (A9647, Sigma Aldrich, St. Louis, USA) for at least one and a half hour at RT to prevent unspecific protein binding.

Following the blocking step, the cells were incubated with a patient sample dilution overnight at 4°C in a humidified chamber. The patient samples were diluted in 10% AB-Diluent, as followed: (1) 2 µl patient serum or plasma was resuspended in 80 µl 10% AB-Diluent (1:40); (2) 20 µl patient CSF were resuspended in 20 µl 10% AB-Diluent (1:2).

On the next day, three wells of a six-well-plate were filled with 1xPBS and the other three wells were filled with demineralized water. After the overnight incubation, the cells were washed three times in 1xPBS.

Cells were then immunolabelled with an Alexa Fluor anti-human IgG secondary antibody (AF594) (A-11014, Gibco, Thermo Fisher Scientific; Waltham, USA) (1:750 in 10% AB-Diluent) for 30 min at RT in a humidified chamber in the dark. A fluorescent-conjugated secondary goat anti-rabbit Cy3 antibody (111-165-144, Jackson Immuno Research; Pennsylvania, USA) was used for the commercial positive control. Afterwards, the cells were washed three times in 1xPBS. For nuclear staining, the cells were incubated with 4´,6-diamidino-2-phenylindole (DAPI; 1 µg/ml) (D1306, Invitrogen; Carlsbad, USA) (diluted in 1xPBS) for one to three min in a humidified chamber in the dark. Then, the cells were washed three times in demineralized water and mounted with one drop of a tip of Aqua-Poly/Mount (18606-20, Polysciences; Warrington, USA) onto glass slides. The slides were stored at 4°C for at least two hours, until the analysis (described in section 3.4.5) was performed.

3.4.5 Analysis – fixed cell-based assay

Microscopic examination and fluorescent images of the anti-GFAPα CBA were performed using an OLYMPUS BX63 fluorescence microscope. Autoantibodies against the α-subunit of GFAP result in a characteristic immunofluorescent pattern with a prominent staining of the cell body. The ANA's control showed strong nuclear staining.

3.5 Anti-neuronal tissue-based assay (anti-neuronal TBA)

Patient's serum, plasma and/or CSF samples were tested for anti-neuronal surface autoantibodies by an in-house TBA (anti-neuronal TBA) on adult rat brain sections via indirect immunohistochemistry (IHC). The following steps were performed with the help of the employees of the NPC, Department of Neurology, Medical University of Vienna.

3.5.1 Preparation

An adult Sprague Dawley rat was sacrificed, the brain was removed from the skull and fixed in 4% PFA for one hour at 4°C. After washing three times in 1xPBS, the brain was incubated in 40% sucrose (1.07651.1000, Merck KgaA; Darmstadt, Germany) solution (diluted in 1xPBS) for two to three days at 4°C for cryoprotection. Then, the brain was embedded in Tissue-Tek O.C.T. compound (optimal cutting temperature compound) (4586, Scigen Scientific; Gardena, USA) and snap frozen in 2-methylbutane (12191502, Honeywell; Muskegon, USA) chilled with liquid nitrogen (0092, Messer SE & Co. KGaA; Bad Soden am Taunus, Germany). Two 8 µm thick rat brain sections were cut, attached to one glass slide by employees of the NPC, Department of Neurology, Medical University of Vienna and stored at -80°C.

3.5.2 Extracellular receptor staining

The glass slides with the rat brain sections were defrosted for 20 min at RT and labelled. Each brain section was surrounded with a hydrophobic Pen (Dako). Afterwards, the slides were placed in a cuvette, filled with 1xPBS, and placed on a rocking platform (Gesellschaft für Labortechnik mbH (GFL)) for five min. 0.3% hydrogen peroxide was diluted in one part 30% H_2O_2 (K48743809, Millipore; Massachusetts, USA) and 99 parts 1xPBS. The slides were incubated with 0.3% H_2O_2 in the cuvette on the rocking platform for exactly 15 min. The incubation was followed by three washing steps in 1xPBS on the rocking platform, 5 min each. The washed slides were placed in a humidified chamber. Each brain section was covered with 200 µl 5% blocking solution (normal donkey serum (566460, Millipore, Massachusetts, USA) (diluted 1:20 in 1xPBS). The brain sections were incubated with the blocking solution for at least 1.5 hours in the humidified chamber.

Afterwards, blocking solution was removed and diluted patient sample was added to the rat brain sections and incubated overnight in a humidified chamber at 4 to 8°C. For the

dilution, 1 µl patient serum or plasma was resuspended in 200 µl blocking solution (1:200). A total of 75 µl patient CSF were resuspended in 75 µl blocking solution (1:2).

On the following day, slides were washed three times in 1xPBS in a cuvette on the rocking platform for five min each. The secondary antibody staining was performed automatically with the Autostainer Link 48 system (Dako/Agilent, Santa Clara, USA). Therefore, a biotinylated donkey anti-human secondary IgG antibody (709-065-149, Jackson Immuno Research; Pennsylvania, USA) was used and diluted 1:2000 in 10% AB-Diluent. After the incubation with the secondary antibody, the rat brain sections were incubated with a Streptavidin/horseradish peroxidase (HRP) (K0675, Dako/Agilent; Santa Clara, USA) complex, which bound to the biotinylated secondary antibody. Then, the chromogen 3,3'-Diaminobenzidine (DAB) (K3468, Dako/Agilent, Santa Clara, USA) was added, resulting in a brown precipitate (staining) on the rat brain sections.

Afterwards, the sections were dehydrated with 50%, 70%, 80%, 96% ethanol, and with n-butyl acetate (K52982952, Supelco, Pennsylvania, USA) and finally mounted either automatically with a Microm CTM Glass Coverslipper (Gibco, Thermo Fisher Scientific), or manually. The analysis of the TBA was performed using a light microscope (Nikon Eclipse E400).

4 Results

4.1 Interpretation of patient data

4.1.1 Gender and age distribution

In total, 450 patients were included in this study. Based on our inclusion criteria, patients with an available autopsy and CSF and/or serum/plasma samples between the year 2000 and September 2021 were included. First, we analyzed the gender and age distribution of included patients, which is illustrated in **Figure 8**. The gender distribution among the included patients showed a slight female predominance with 54% of patients (241/450) (male 46%, 209/450 patients), F:M ratio 1.2:1, as illustrated in **Figure 8A**. The age distribution is shown in **Figure 8B**. A total of 2% of patients (8/450) were 18 years old or younger. A third (33%) of the patient cohort (148/450) was between the age of 19 and 65 years and the majority (65%) of patients were older than 65 years (294/450).

In a second step, we looked at the available clinical data of all included patients (see section 4.1.2).
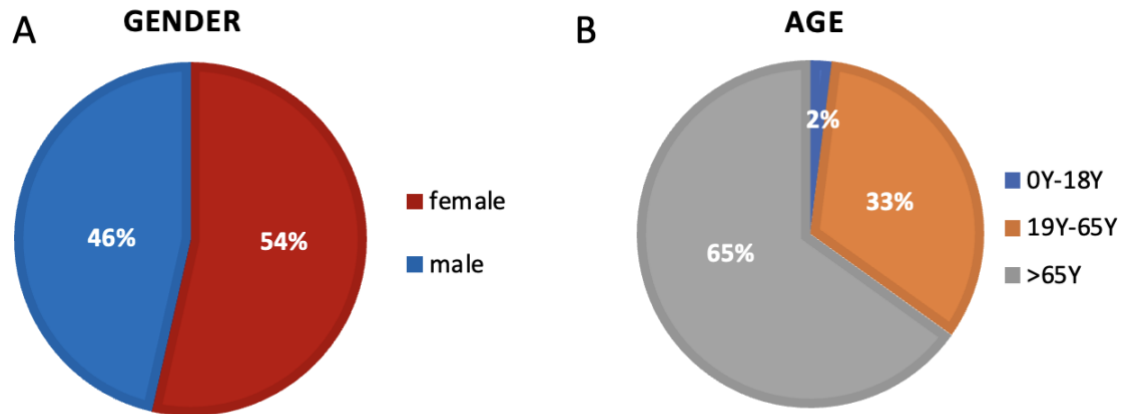
Figure 8: Gender and age distribution of the included patients. **(A)** F(red):M(blue) ratio is 1.2:1, showing a slight female predominance. **(B)** 2% of patients (8/450) were under 19 years old (blue). 33% of patients (148/450) were between the age of 19 and 65 years old (orange). The majority of patients (294/450), 65%, were older than 65 years (grey). Y= years

4.1.2 Interpretation of clinical data

Clinical data including symptoms, morbidities, cause of death, and autopsy reports were collected and analyzed from all patients who met the inclusion criteria. In the majority of the patient cohort, more than one disease was diagnosed in one patient. This might be explained by the fact that multimorbidity is a common occurrence in patients over 65 years of age, who made up the bulk of our patient cohort (see **Figure 8B**). Therefore, only "primary" diseases relevant to this study were selected (see **Figure 9**), and if a patient had comorbidities along with the underlying primary disease, the primary diseases were prioritized as follows: Creutzfeldt Jakob Disease (CJD) > neurodegenerative disease > others; for example, if a patient was diagnosed with both CJD and a neurodegenerative disease, the patient was only listed in the CJD category. Antibody-associated autoimmune encephalitis (AIE) > encephalitis/meningitis/meningo-encephalitis/meningo-encephalomyelitis > primary neoplasia > viral infection > others; for instance, a patient with antibody-associated AIE was listed in its category, even if a tumor was diagnosed in this patient. The distribution of prioritized primary diseases that were diagnosed in the included patients is shown in **Figure 9**.

Almost 50% of patients (222/450) were diagnosed with CJD. The increased number of autopsies in this field can be explained by the fact that the NPC, Department of Neurology, Medical University of Vienna, is the Austrian Reference Center for Prion Diseases and suspected prion cases.

The second largest group with almost 15% of patients (66/450) included those with neurodegenerative diseases. Neurodegenerative diseases in this study included Alzheimer's disease (AD) in 70% of patients (46/66), Lewy-body-dementia (LBD) in 17% of patients (11/66), and argyrophilic grain disease in 14% of patients (9/66).

4.4% of included patients (20/450) were diagnosed with an antibody-associated AIE, which is illustrated in **Figure 9**. We further analyzed the distribution of these anti-neuronal and anti-glial antibody-associated AIEs diagnosed in included patients. The detected autoantibodies of the patients diagnosed with this disorder are shown in **Figure 11**.

In some patients diagnosed with encephalitis, meningitis, meningo-encephalitis, or meningo-encephalomyelitis, an underlying tumor was identified, and their distribution is illustrated in **Figure 10**. A total of 2.4% of patients (11/450) were diagnosed with encephalitis, 36.4% of whom (4/11) were accompanied by an underlying tumor.

Meningitis was diagnosed in 0.4% of patients (2/450), 50% of whom (1/2) had an underlying tumor. Meningo-encephalitis was diagnosed in 1.3% of patients (6/450), 50% of whom (3/6) were accompanied by an underlying tumor. Meningo-encephalomyelitis was diagnosed in 0.2% of patients (1/450), none of whom had an underlying tumor. The sample material (CSF, serum, and/or plasma) of patients associated with these diseases showed no signs of either well characterized high-risk autoantibodies (intracellular antigens e.g., ANNA-1, ANNA-2, PCA-1, Tr, CV2, Amphiphysin, Ma1/2, PKCgamma, CARPVIII, ARHGAP26), or tumor- (SOX1) and non-tumor-associated autoantibodies (GAD65, AK5, Homer3). Moreover, screening for surface receptor/synaptic autoantibodies did not show a hippocampal neuropil staining pattern in the anti-neuronal TBA, which would be typical for autoantibodies against NMDAR, AMPAR, GABA(B)R, LGI1, or CASPR2, as well as nodal/paranodal antigens (NF155, CNTN1, CASPR1). Nevertheless, these negative test results do not exclude an autoimmune mediated neurological syndrome of other origin.

As illustrated in **Figure 9**, 6.7% of the patient cohort (30/450) were diagnosed with a primary neoplasia, such as adenocarcinoma, breast cancer, choriocarcinoma, glioblastoma, gliofibroma, Hodgkin lymphoma, non-Hodgkin lymphoma, and meningioma. In addition, no autoantibodies against anti-neuronal surface/synaptic, anti-glial (AQP4, MOG), or intracellular antigens were detected in these patients.

Viral infection occurred in 15.6% of included patients (7/450), 57.1% of whom (4/7) were diagnosed with progressive multifocal leukoencephalopathy (PML), and 14.3% each were diagnosed with tick-borne encephalitis (TBE) (1/7), human immunodeficiency virus (HIV) (1/7), or Epstein-Barr Virus antibodies (EBV) (1/7).

18.9% of patients (85/450) were diagnosed with other diseases such as metabolic diseases, amyotrophic lateral sclerosis (ALS), or cerebral edemas, which were not relevant for this study and were therefore combined into one category.
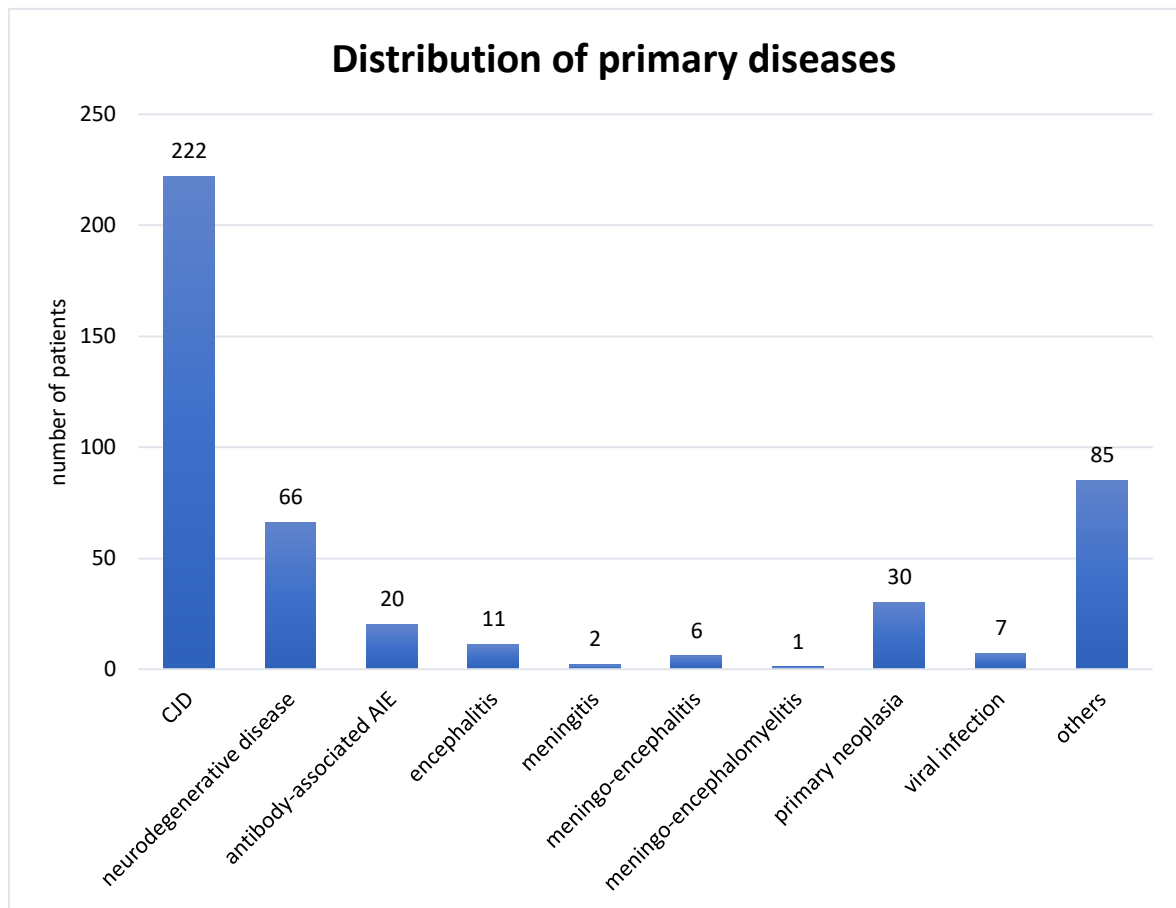
Figure 9: Distribution of primary diseases in the patient cohort. 222 patients (222/450) were diagnosed with Creutzfeldt Jakob disease (CJD), and 66 patients (66/450) with a neurodegenerative disease, such as Alzheimer's disease (AD), Lewy-body-dementia (LBD) or argyrophilic grain disease. 20 patients (20/450) were diagnosed with an antibody-associated AIE. 11 patients (11/450) were diagnosed with encephalitis, two with meningitis (2/450), six with meningo-encephalitis (6/450), and one patient with meningo-encephalomyelitis (1/450). 30 patients (30/450) had a primary neoplasia. A viral infection occurred in seven patients (7/450). 85 patients (85/450) had other diseases, such as metabolic diseases, ALS, and cerebral edemas. AIE= autoimmune encephalitis, ALS= amyotrophic lateral sclerosis, CJD= Creutzfeldt Jakob disease.
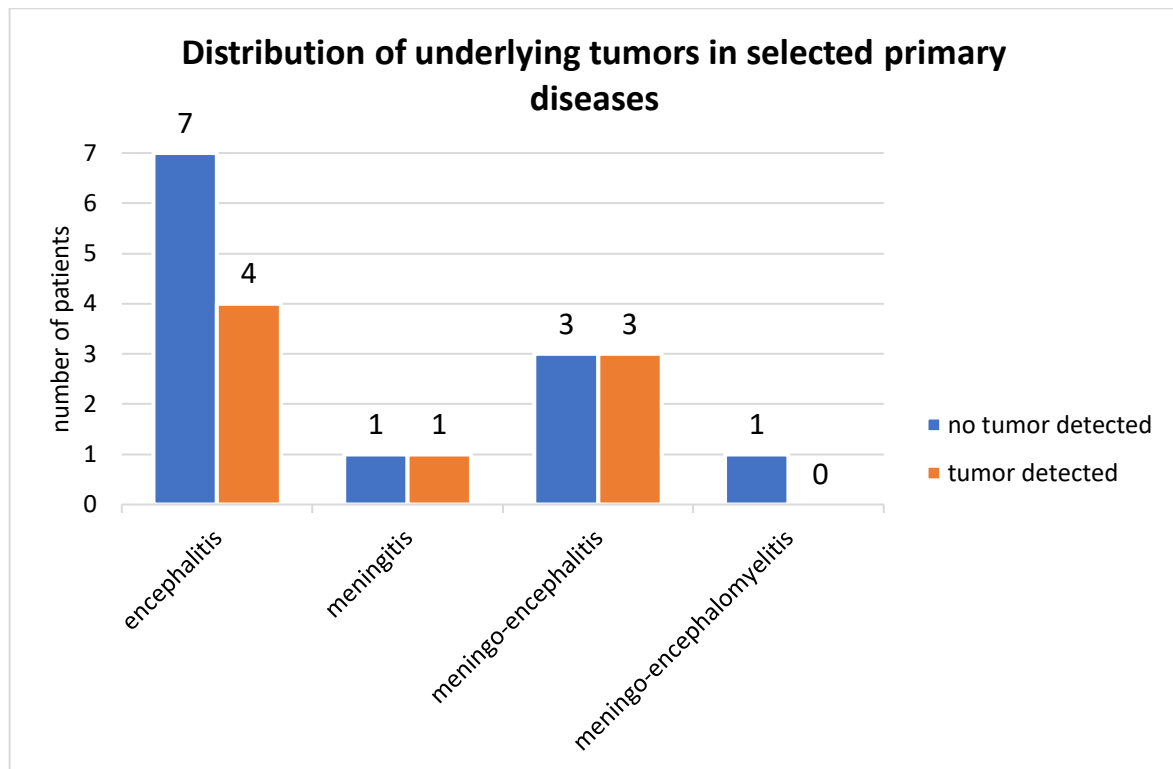
Figure 10: Distribution of underlying tumors in patients with encephalitis, meningitis, meningo-encephalitis, and meningo-encephalomyelitis. Four patients (4/11) diagnosed with encephalitis, one patient (1/2) with meningitis, three patients (3/6) with meningo-encephalitis, and no patient (0/1) with meningo-encephalomyelitis had an underlying tumor. Orange= tumor detected, Blue= no tumor detected.

Next, since concomitant autoantibodies, particularly anti-NMDAR, can occur in patients with GFAP meningo-encephalomyelitis (see section 1.3.7), we examined all 20 antibody-associated AIE patients and their detected autoantibodies (see **Figure 11**). Moreover, a paraneoplastic event, particularly an ovarian teratoma (see section 1.3.2), can be observed in 22% of patients with GFAP meningo-encephalomyelitis [43]. Therefore, we examined whether a paraneoplastic event could be observed in included patients (see **Figure 12**).

As illustrated in **Figure 11**, antibody-associated AIE can be roughly divided into two categories: (1) autoantibodies directed against intracellular neuronal antigens, and (2) autoantibodies directed against neuronal surface or synaptic antigens. Antineuronal nuclear antibodies type 1 (ANNA-1) ("anti-Hu"), antineuronal nuclear antibodies type 2 (ANNA-2) ("anti-Ri"), Purkinje cell antibodies type 1 (PCA-1) ("anti-Yo"), Amphiphysin, and Ma2 belong to the intracellular neuronal antigens. Taking a closer look, the largest group with 20% of AIE patients (4/20) had autoantibodies against ANNA-1, while 5% of AIE

patients each had autoantibodies against ANNA-2 (1/20), amphiphysin (1/20), PCA-1 (1/20), and Ma2 (1/20).

Autoantibodies directed against surface or synaptic antigens include α-amino-3-hydroxy-5-methyl-4-isoxazolepropionic acid receptor (AMPAR), Aquaporin4 (AQP4), contactin-associated protein-2 (CASPR2), contactin 1 (CNTN1), immunoglobulin-like cell adhesion molecule 5 (IgLON5), leucine rich glioma inactivated 1 (LGI1), myelin oligodendrocyte glycoprotein (MOG), and N-methyl-D-aspartate receptor (NMDAR). Regarding these autoantibodies, 10% of AIE patients each had detected autoantibodies directed against IgLON5 (2/20), MOG (2/20), or NMDAR (2/20), while 5% of patients each exhibited autoantibodies against AMPAR (1/20), AQP4 (1/20), CASPR2 (1/20), CNTN1 (1/20), or LGI1 (1/20).

In one patient with antibody-associated AIE, the antigen remains unknown as all previously described antigens were negative in the CBA, but the anti-neuronal TBA showed a positive neuropil staining pattern and a positive staining of live neurons could be observed suggesting an autoimmune-associated neurological syndrome of other origin.
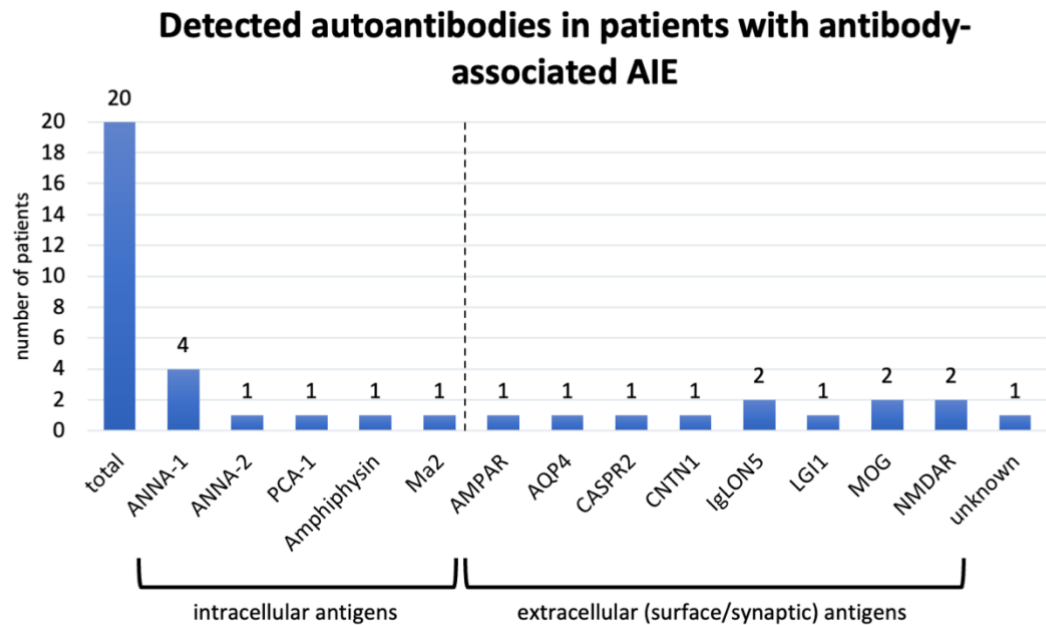
Figure 11: Autoantibodies detected in patients with antibody-associated AIE. Autoantibodies can be directed against intracellular neuronal (to the left of the dashed line), and extracellular surface/synaptic antigens (to the right of the dashed line). Autoantibodies directed against the intracellular antigen ANNA-1 were detected in 20% of patients (4/20). All other patients in this category with autoantibodies directed against

ANNA-2 (1/20), PCA-1 (1/20), Amphiphysin (1/20), and Ma2 (1/20) were detected in one patient each. The autoantibodies against the surface/synaptic antigens AMPAR (1/20), AQP4 (1/20), CASPR2 (1/20), CNTN1 (1/20), and LGI1 (1/20) were detected in one patient each. Autoantibodies against IgLON5 (2/20), MOG (2/20), and NMDAR (2/20) were detected in two patients each. The antigen of one patient (1/20) with antibody-associated AIE remains unknown. AIE= autoimmune encephalitis, AMPAR= α-amino-3-hydroxy-5-methyl-4-isoxazolepropionic acid receptor, ANNA-1= antineuronal nuclear antibodies type 1, ANNA-2= antineuronal nuclear antibodies type 2, AQP4= Aquaporin 4, CASPR2= contactin-associated protein-2, CNTN1= contactin1, IgLON5= immunoglobulin-like cell adhesion molecule 5, LGI1= leucine rich glioma inactivated 1, MOG= myelin oligodendrocyte glycoprotein, NMDAR= N-methyl-D-aspartate receptor, PCA-1= Purkinje cell antibodies type 1.

Antibody-associated AIE can be associated with a paraneoplastic event, which can occur particularly in patients who have autoantibodies against intracellular neuronal antigens. Therefore, we further analyzed all 20 AIE patients for a potential paraneoplastic event, which is illustrated in **Figure 12**.

Overall, paraneoplastic events in patients with antibody-associated AIE were diagnosed in 50% of included patients (10/20), which is shown in **Figure 12**. Interestingly, all patients (8/8) with autoantibodies directed against intracellular neuronal antigens were associated with a paraneoplastic event. Underlying tumors were for example breast cancer (1/8), colorectal cancer (1/8), lung cancer (3/8), and squamous cell carcinoma (1/8).

In patients with autoantibodies that target the surface or synapse, an underlying tumor was found in 16.7% of patients (2/12). Lung cancer was identified in one patient (1/1) associated with autoantibodies against LGI1, while one patient with NMDAR autoantibodies (1/2) was diagnosed with a lymphoma.
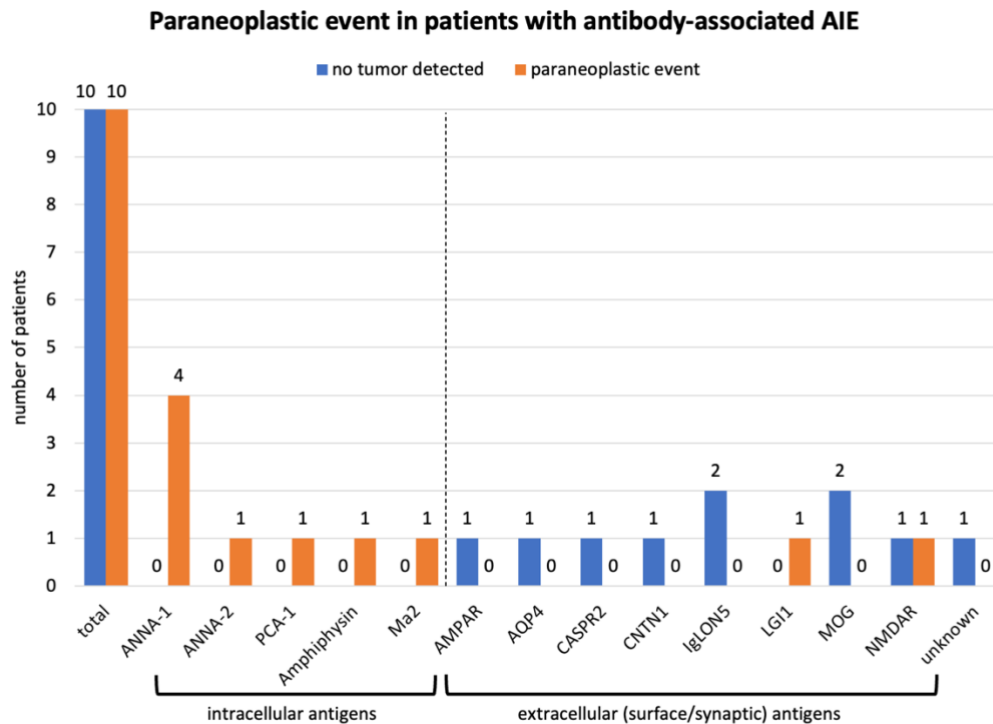
Figure 12: The distribution and occurrence of paraneoplastic events in patients with antibody-associated AIE. Overall, a paraneoplastic event was identified in 50% of patients (10/20) (orange), while no tumor was diagnosed in the other 50% of patients (10/20) (blue). All patients (8/8) with detected autoantibodies directed against the intracellular neuronal antigens ANNA-1 (4/4), ANNA-2 (1/1), PCA-1 (1/1), amphiphysin (1/1), and Ma2 (1/1) were accompanied by an underlying tumor (8/8). A paraneoplastic event was diagnosed in 16.7% of patients (2/12) with autoantibodies to surface/synaptic antigens, including one patient with anti-LGI1 IgG (1/1) and one patient with anti-NMDAR IgG (1/2). All other patients (10/12) with detected surface/synaptic-targeting autoantibodies (AMPAR (1/1), AQP4 (1/1), CASPR2 (1/1), CNTN1 (1/1), IgLON5 (1/1), MOG (1/1), NMDAR (1/2)) were not associated with a paraneoplastic event. The patient with detected autoantibodies against a previously unknown antigen had no underlying tumor. AIE= autoimmune encephalitis, AMPAR= α-amino-3-hydroxy-5-methyl-4-isoxazolepropionic acid receptor, ANNA-1= antineuronal nuclear antibodies type 1, ANNA-2= antineuronal nuclear antibodies type 2, AQP4= Aquaporin 4, CASPR2= contactin-associated protein-2, CNTN1= contactin1, IgLON5= immunoglobulin-like cell adhesion molecule 5, LGI1= leucine rich glioma inactivated 1, MOG= myelin oligodendrocyte glycoprotein, NMDAR= N-methyl-D-aspartate receptor, PCA-1= Purkinje cell antibodies type 1.

4.2 Screening for anti-GFAPα autoantibodies

4.2.1 Available sample material

From this patient cohort, a total of 599 patient samples from 450 included patients were screened for anti-GFAPα IgG autoantibodies. Different patient sample material was available for screening. A total of 33% of patients (148/450) had both CSF and serum samples available, which is shown in **Figure 13**. In addition, 45% of patients (200/450) had

only CSF available for screening, 21% of patients (96/450) only serum, and 1% of patients (6/450) only plasma. The samples were screened for anti-GFAPα IgG autoantibodies using a HEK293T fixed CBA.
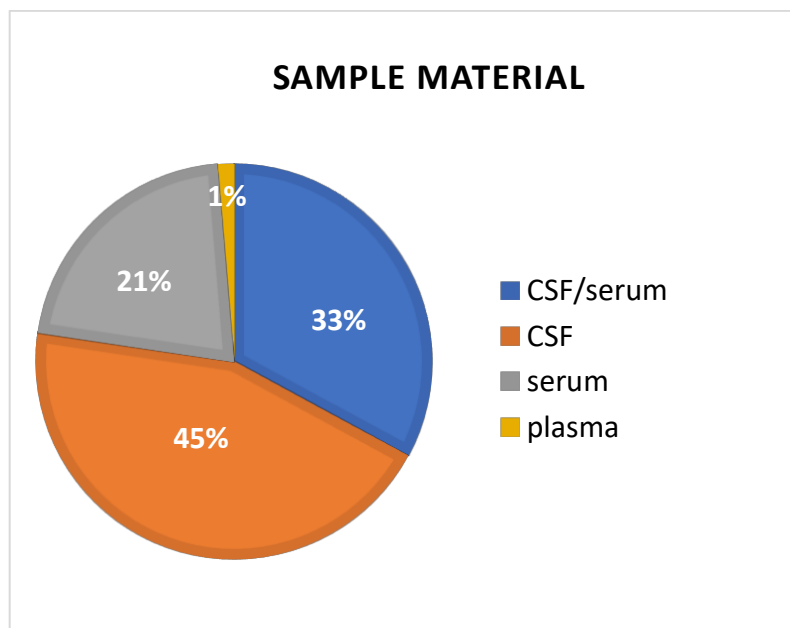

Figure 13: Available sample material of the included patients. 33% of patients (148/450) had both CSF and serum (blue), 45% of patients (200/450) had only CSF (orange), 21% of patients (96/450) had only serum (grey), and 1% of patients (6/450) had only plasma (yellow) available for anti-GFAPα screening. CSF= cerebrospinal fluid

4.2.2 Evaluation of anti-GFAPα screening

As described in section 4.2.1, 599 samples of 450 patients were screened for anti-GFAPα IgG autoantibodies. As a screening method, a fixed CBA with HEK293T cells expressing GFP-tagged GFAPα was performed, which is described in section 3.4. The CBAs were evaluated using an OLYMPUS BX63 fluorescence microscope, which is illustrated in **Figure 14**.

A healthy human negative control is illustrated in **Figure 14A-C**, where no anti-GFAPα IgG autoantibodies were detected in the CBA, as transfected and AF594 immunostained cells did not overlap.

Immunostaining of a human positive control is demonstrated in **Figure 14D-F**, where the presence of anti-GFAPα IgG autoantibodies could be detected due to an overlap in transfected and AF594 immunostained cells.

The presence of anti-GFAPα IgG autoantibodies in the commercial positive control is shown in **Figure 14G-I**. The commercial positive control was immunostained with a

fluorescent-conjugated Cy3 secondary antibody (see **Figure 14H**). Very similar positive immunostaining and transfection overlap could be observed compared to the human positive control (see **Figure 14F**) but a different secondary antibody fluorescent conjugate was used (see **Figure 14I**).
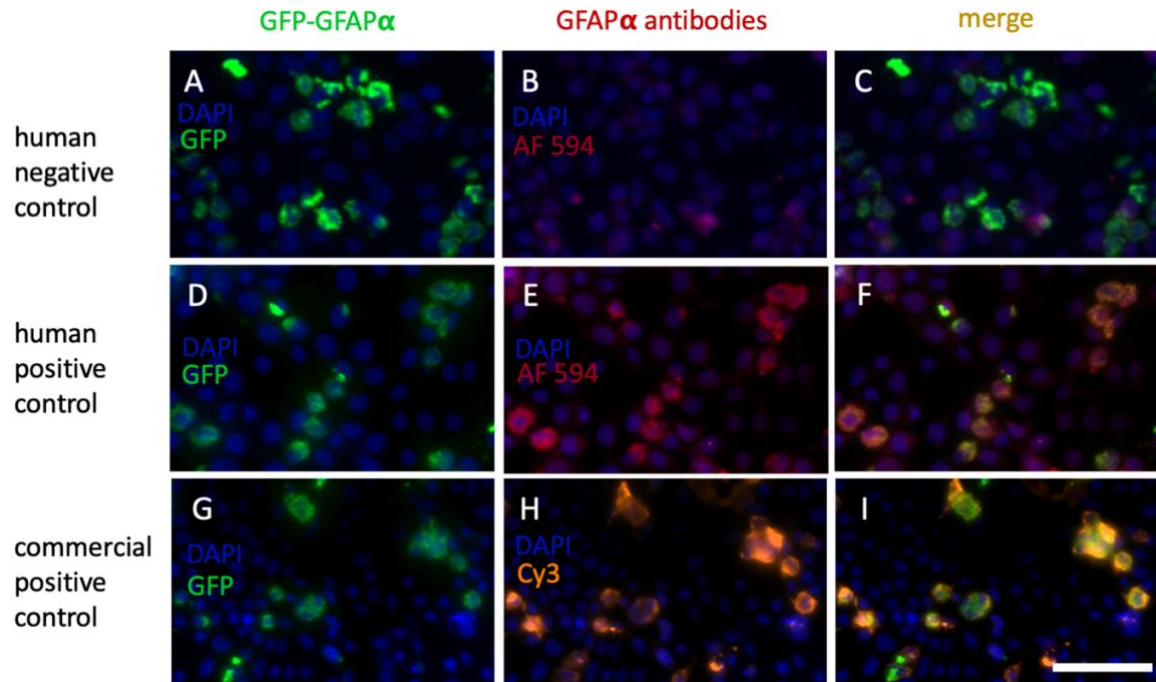

Figure 14: Screening for anti-GFAPα autoantibodies on transfected HEK293T cells in three different controls. HEK293T cells expressing the GFP-tagged GFAPα plasmid (green) were immunostained with anti-GFAPα human (AF594, red) **(A-F)** or rabbit (Cy3, orange) **(G-I)** IgG. Cell nuclei were stained with DAPI (blue). Since GFAP is an intracellular protein, a characteristic immunofluorescence staining pattern with a prominent staining of the cell body was expected. **(A, D, G)** illustrate the GFAPα transfected HEK293T cells (GFP, green) with a nuclear DAPI staining (blue). **(B, E, H)** indicate the presence of anti-GFAPα IgG autoantibodies immunolabelled with the appropriate secondary antibody (AF594 or Cy3). **(C, F, I)** show merge images of transfected and IgG positive immunostained cells (yellow). A human negative control is illustrated in **(A-C)**, which demonstrates no presence of anti-GFAPα IgG autoantibodies. IgGs from a human positive control are shown in **(D-F)** and demonstrate a yellow overlap **(F)** with AF594 immunostained (red) and transfected (green) cells. Commercial positive control is shown in **(G-I)** demonstrating the presence of anti-GFAPα IgG autoantibodies with a bright yellow overlap of Cy3 immunostained (orange) and transfected (green) cells. Scale bar: 50 µm. DAPI= 4´,6-diamidino-2-phenylindole, GFAP= glial fibrillary acidic protein, GFP= green fluorescent protein.

A higher magnification and a more detailed view of HEK293T cells stained with the human positive control are shown in **Figure 15,** taken with a 100x objective using the fluorescence microscope. Overlap of GFAPα expression and immunostaining in four cells is demonstrated, indicating a binding of anti-GFAPα IgG autoantibodies to the target antigen GFAPα.
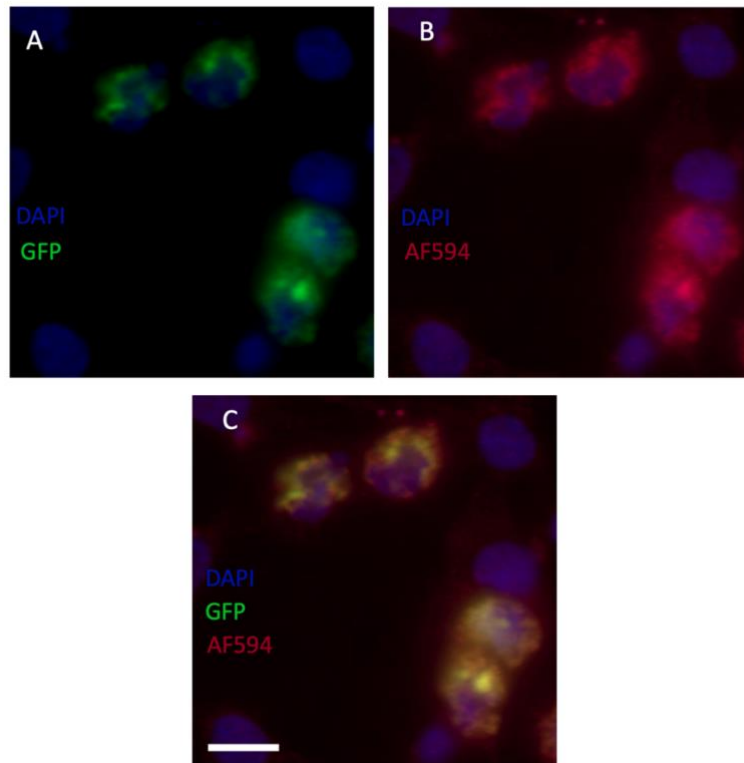
43

Figure 15: A detailed overview of a positive anti-GFAPα IgG autoantibody staining using a human positive control. The cell nuclei were stained with DAPI (blue). **(A)** The GFAPα expression (GFP, green) in the cell and **(B)** the AF594 fluorescent-conjugated immunostaining (red) were present in four cells. **(C)** illustrates the merged image of **(A)** and **(B)** with an overlap (yellow) of GFAPα expression within the cell (green) and a positive immunostaining (red) in four cells. Scale bar: 10 µm. DAPI= 4´,6-diamidino-2-phenylindole, GFAP= glial fibrillary acidic protein, GFP= green fluorescent protein.

After screening 599 samples from 450 patients for anti-GFAPα IgG autoantibodies via a fixed CBA, no positive staining was found in any of these patients. This leads to the result that 100% of all screened patients showed no presence of anti-GFAPα IgG autoantibodies in CSF, serum, and/or plasma, which is illustrated in **Figure 16**.
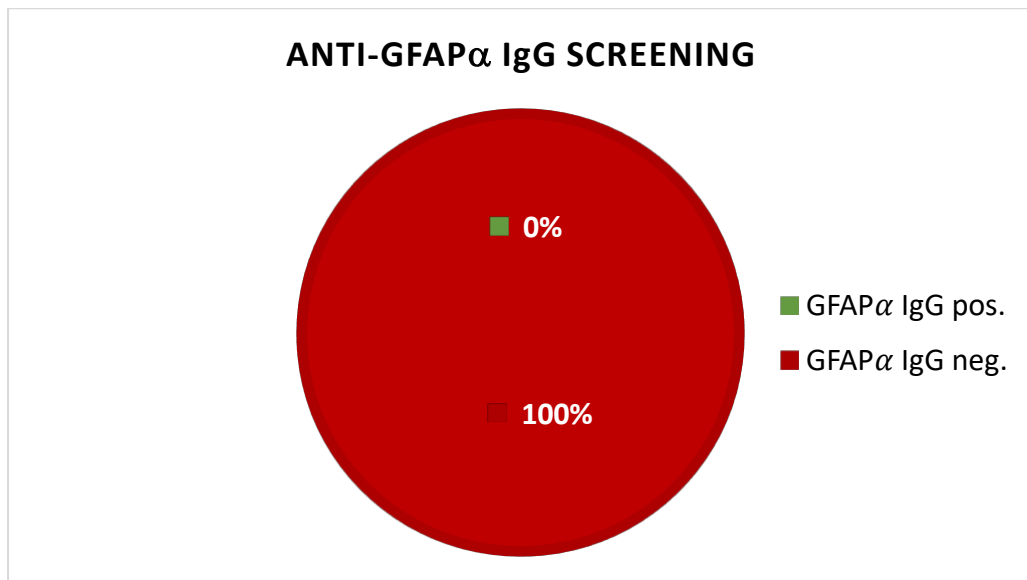
Figure 16: Results of anti-GFAPα IgG autoantibody screening via a fixed cell-based assay. None of the screened patients (green) showed an anti-GFAPα IgG autoantibody positive staining in CSF, serum and/or plasma. Green= GFAPα IgG positive, red= GFAPα IgG negative. IgG= Immunoglobulin G, GFAP= glial fibrillary acidic protein.

4.3 Positive astrocyte staining in anti-neuronal tissue-based assay

Since none of the included patients had anti-GFAPα IgG autoantibodies, we carried out a second additional project. In this project, all patients who showed a specific astrocyte staining pattern in the anti-neuronal TBA (see section 3.5) were tested for anti-GFAPα IgG autoantibodies.

In 2018 Shan et al. reported a characteristic immunofluorescence (IF) staining pattern on frozen murine brain tissue from a patient sample with anti-GFAPα IgG autoantibodies. They detected a positive astrocyte staining in the hippocampus and a Bergmann radial glial pattern in the cerebellum [42]. While Shan et al. detected these characteristic staining patterns via IF, a specific astrocyte staining (see **Figure 17)**, particularly in the hippocampus and cerebellum, could also found in an in-house anti-neuronal TBA on adult rat brain via indirect IHC, which was analyzed using a light microscope. This particular staining pattern was found in some of the routinely tested patients at the NPC, Department of Neurology, Medical University of Vienna. Interestingly, many positively stained astrocytes were visible in and around the hippocampus (see **Figure 17B**) in these patients. A more detailed view of the cerebellum is illustrated in **Figure 17C**, showing a prominent radial Bergmann glial cell staining pattern. A higher magnification of positively stained astrocytes in the cerebellum is shown in **Figure 17D.**

Next, we wanted to investigate whether there is a potential correlation between positive astrocyte staining in anti-neuronal TBA and the presence of anti-GFAPα IgG autoantibodies in CBA in patient samples.
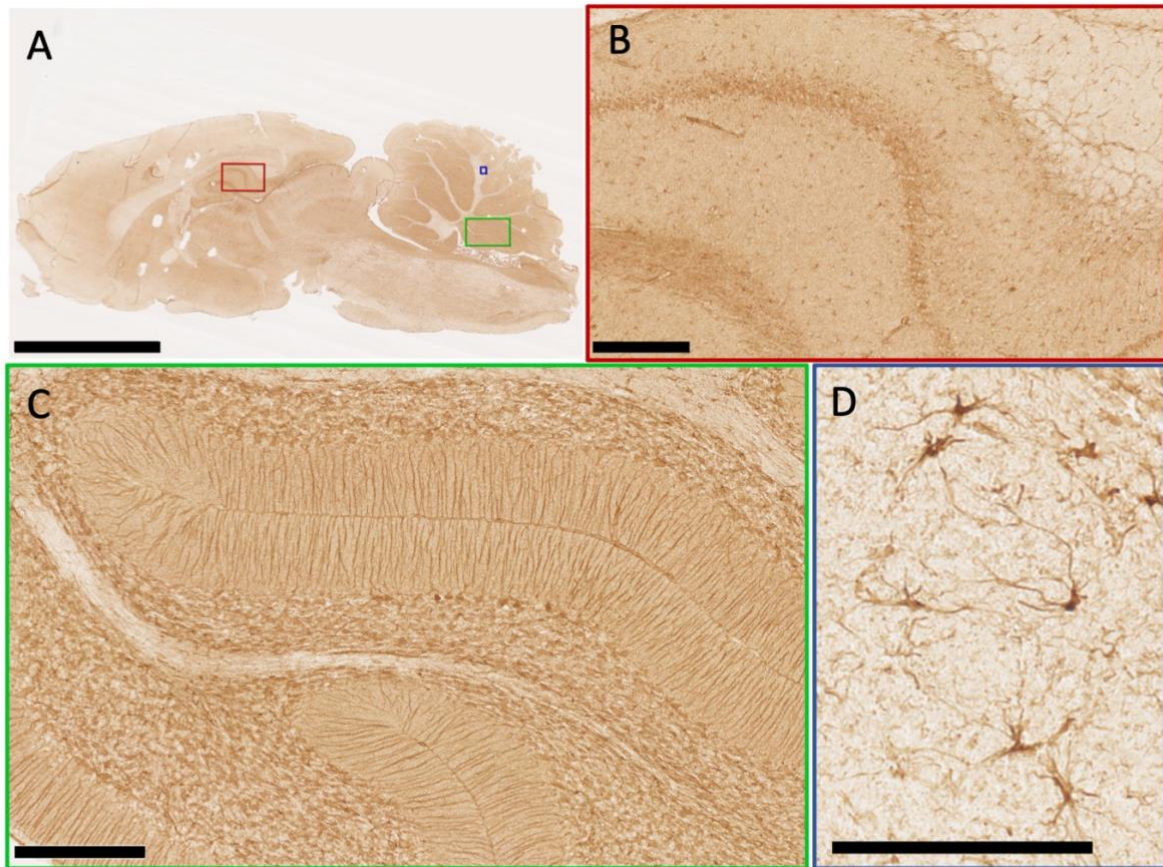
Figure 17: Specific astrocyte staining pattern of an in-house anti-neuronal tissue-based assay using indirect immunohistochemistry on frozen adult rat brain sections. **(A)** The overview of an immunostained (brown) rat brain section is demonstrated. Red rectangle enlarged in panel **(B)**: The immunostained hippocampus is illustrated in more detail showing stained astrocytes (brown) in and around the hippocampus. Green rectangle enlarged in panel **(C)**: Detailed illustration of the cerebellum with a characteristic radial glial pattern and astrocyte staining in different layers are shown. Blue rectangle enlarged in panel **(D)**: Astrocyte staining (brown) apparent in the white matter of the cerebellum is shown in detail. Scale bar **(A)**: 5 mm; scale bar **(B, C)**: 250 μm, scale bar **(D)**: 100 μm.

4.3.1   Patient information

The second project included CSF and/or serum samples from 31 patients collected between the year 2019 and October 2021. Patients with various primary diseases such as pediatric-onset multiple sclerosis (POMS), or with a diagnosed lung cancer, were included in this study if an astrocyte staining pattern was observed in the anti-neuronal TBA in at least one patient sample and anti-GFAPα CBA had not been performed at that time.

First, we analyzed the gender and age distribution of all included patients (see **Figure 18**). The gender distribution among patients with an astrocyte staining in anti-neuronal TBA is shown **Figure 18A**. Patient data were not available for 3% of patients (1/31), therefore gender could not be identified. The majority of patients (17/31) were male with 55% and 42% female (13/31), M:F ratio: 1.3:1.

The age distribution is shown in **Figure 18B**. The age of 6% of patients (2/31) remains unknown as these data were not available in "KINNet", an internal patient database provided by the NPC based. The smallest group included one patient under 19 years of age, accounting for 3% of all patients (1/31). The largest group included patients between the age of 19 and 65 years with 65% of patients (20/31). 26% of patients (8/21) older than 65 years showed an astrocyte staining in anti-neuronal TBA.
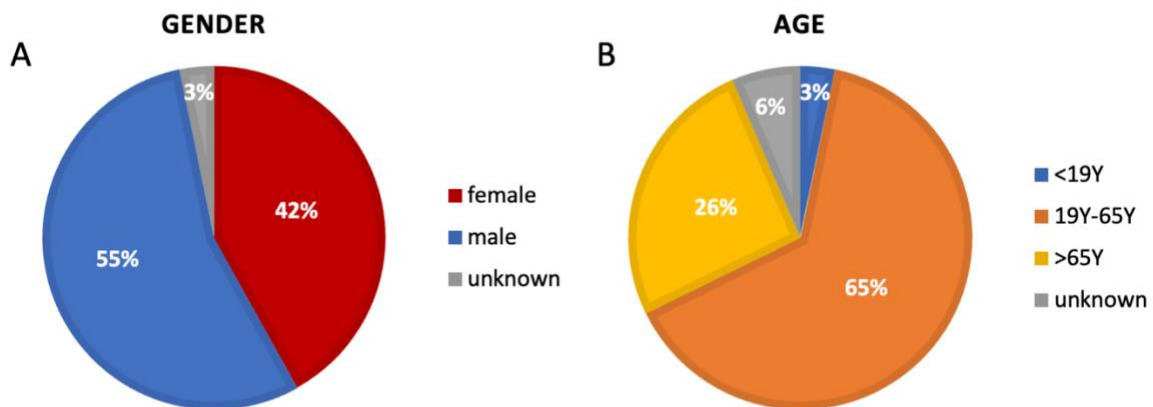

Figure 18: Gender and age distribution of patients with an astrocyte staining in anti-neuronal TBA. **(A)** M(blue):F(red) ratio is 1.3:1, showing a slight male predominance. In 3% of patients, the gender was unknown (grey). **(B)** 3% of patients were under 19 years (blue), 65% were between 19 and 65 years (orange), 26% were older than 65 years (yellow), and 6% of patient's age were unknown (grey).

4.3.2 Screening for anti-GFAPα autoantibodies

After collecting and analyzing patient data, all available patient samples presenting an astrocyte staining in anti-neuronal TBA in at least one sample were used for CBA. In total, 60 patient samples, including CSF and/or serum, were screened for anti-GFAPα IgG autoantibodies. The distribution of the sample material among included patients is shown in **Figure 19**. 45% of patients (14/31) had only serum available, and 32% of patients (10/31) only CSF. 23% of patients (7/31) had both serum and CSF available.
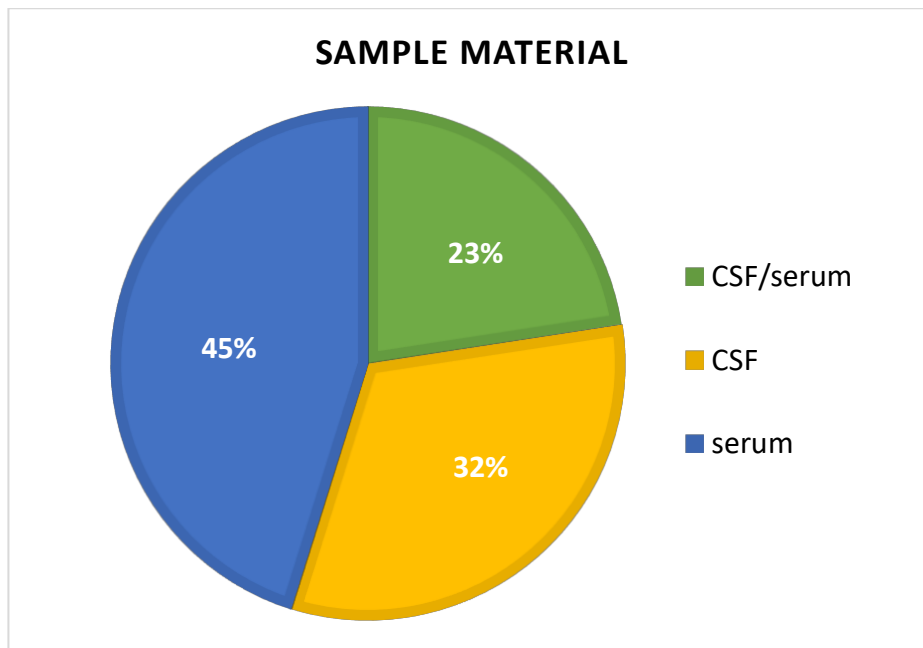
Figure 19: Distribution of sample material in patients with astrocyte staining. 45% of patients only had serum (blue) and 32% only CSF (yellow) available. 23% had both serum and CSF (green) available. CSF= cerebrospinal fluid

Screening of 60 patient samples from 31 patients for anti-GFAPα IgG autoantibodies using a fixed CBA resulted in a positive staining in 3% of patients (1/31), while 97% of patients were negative for anti-GFAPα (30/31), as described in **Figure 20**.
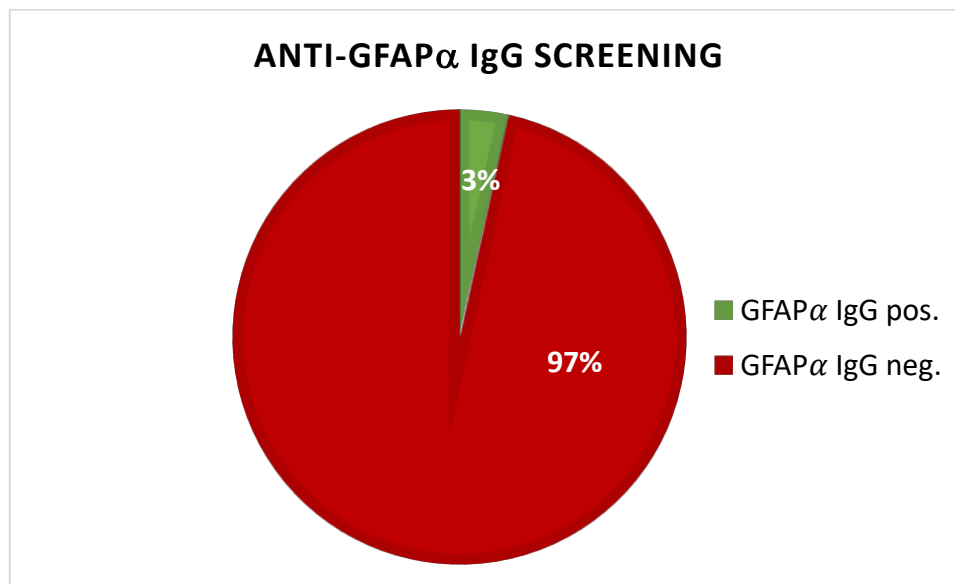

Figure 20: Result of anti-GFAPα IgG autoantibody screening using fixed CBA from patients with astrocyte staining in anti-neuronal TBA. 3% of patients showed a positive staining for anti-GFAPα IgG autoantibodies (green), while 97% of patients were anti-GFAPα IgG negative (red). Green= GFAPα IgG positive, red= GFAPα IgG negative. GFAP= glial fibrillary acidic protein, IgG= Immunoglobulin G.

4.3.3 Patient positive for anti-GFAPα IgG autoantibodies: a case report

A 20-year-old man came to the emergency ambulance on August 8th, 2021, due to status febrilis, worsening clinical symptoms, and suspected meningitis. Despite persistent coughing, throat irritation, loss of appetite and vomiting, extensive infectious workup was unremarkable. Two days before admission to the hospital, he was treated orally with the antibiotic amoxicillin. Clinical examination showed no anomalies apart from anteflexion in the head and neck area. He was admitted to the hospital on August 12th, where the first lumbar puncture was performed (see **Table 6**). Initial CSF analysis revealed 263 white blood cells (WBCs)/µl (normal: 0-5 WBCs/µl) with predominantly lymphocytes and monocytes, elevated total protein 106 mg/dl (normal: 15-45mg/dl), increased lactate 2.7 mmol/l (normal: 0.6-2.2mmol/l), and normal glucose 55 mg/dl (normal: 40-70 mg/dl), while oligoclonal bands were not detected. Serological parameters of inflammation were not increased. The patient received a combined antiviral and antibiotic therapy with 2 g intravenous (i.v.) ceftriaxone and acyclovir (10 mg/kg body weight) three times a day but he did not respond. MRI at this time showed no abnormalities. Follow-up lumbar puncture was performed on August 17th (see **Table 6**) with similar CSF findings. The number of WBCs increased slightly to 288 cells/µl. CXCL13 was elevated in both CSF samples but is considered a non-specific indication of pathogen-related CSF affection. In addition, the patient presented symptoms of urinary retention and a further MRI showed leptomeningeal gadolinium enhancement in the area of the spinal cord punctum maximum, conus, and cauda medullaris. The patient was then treated with intravenous methylprednisolone (5x500 mg). Interestingly, he rapidly responded, and all clinical symptoms and MRI changes improved. A third lumbar puncture was performed on August 30th (see **Table 6**) showing a significant decrease of WBCs (68 cells/µl) and normal protein levels (43.7 mg/dl).

All submitted CSF samples were routinely tested for surface/synapse targeted anti-neuronal autoantibodies using anti-neuronal TBA. The first CSF sample (Sample ID#1) showed no signs of neuropil or astrocyte staining, as illustrated in **Figure 21A, B**. The second CSF sample (Sample ID#2) was submitted five days after antibiotic and antiviral therapy. Anti-neuronal TBA showed no staining in the hippocampus, but a light astrocyte staining in the cerebellum, without the characteristic radial pattern, as shown in **Figure 21C, D**. The last CSF sample (Sample ID#3) showed an incipient neuropil staining pattern

in the rat brain hippocampus, as illustrated in **Figure 21E**. A characteristic astrocyte staining and a radial glial pattern in the cerebellum were present (**Figure 21F**).
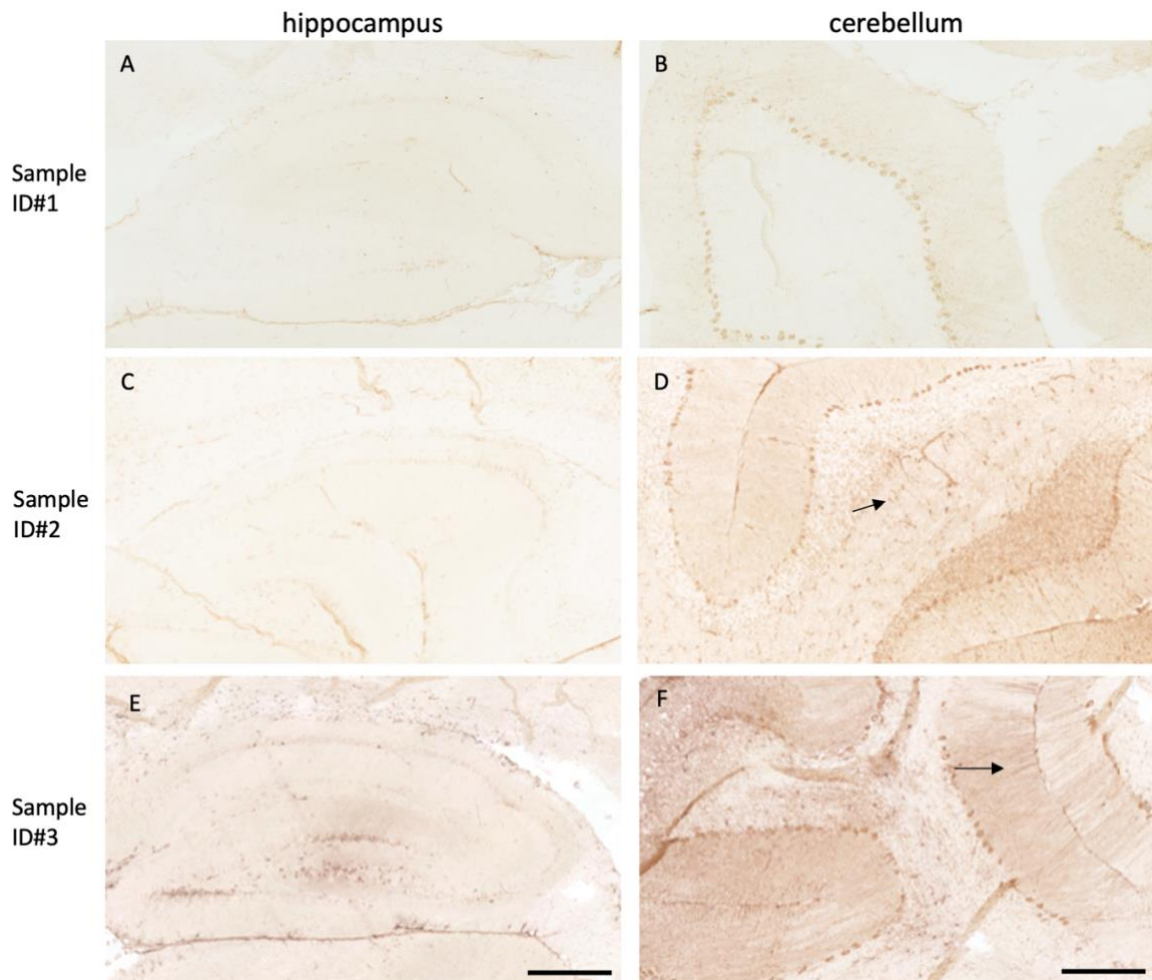

Figure 21: Development of GFAP meningo-encephalomyelitis via anti-neuronal TBA on adult rat brain section in an anti-GFAPα IgG autoantibody positive patient. Sample ID#1 (CSF). **(A, B)** show no staining in the hippocampus or cerebellum. Sample ID#2 (CSF) **(C, D)** show no staining in the hippocampus but some astrocytes with a faint staining in the cerebellum. Arrow in **(D)** indicated positively stained astrocytes. Sample ID#3 (CSF) **(E, F)** show incipient neuropil staining in the hippocampus and astrocyte staining in the hippocampus and cerebellum area. Furthermore, the cerebellum shows a characteristic radial pattern. Arrow in **(F)** indicated a radial glial pattern. Scale bar **(A, C, E)**: 500 μm. Scale bar **(B, D, F)**: 250 μm. CSF= cerebrospinal fluid, GFAP= glial fibrillary acidic protein, IgG= Immunoglobulin G

All CSF samples were tested on anti-GFAPα IgG autoantibodies via fixed CBA, as illustrated in **Figure 22**. Sample ID#3 with an astrocyte staining present in anti-neuronal TBA (see **Figure 21E, F**), showed a slightly positive staining in anti-GFAPα CBA (see **Figure 22G-I)**, while the first two submitted CSF samples were anti-GFAPα IgG negative (see **Figure 22A-C, D-F).**
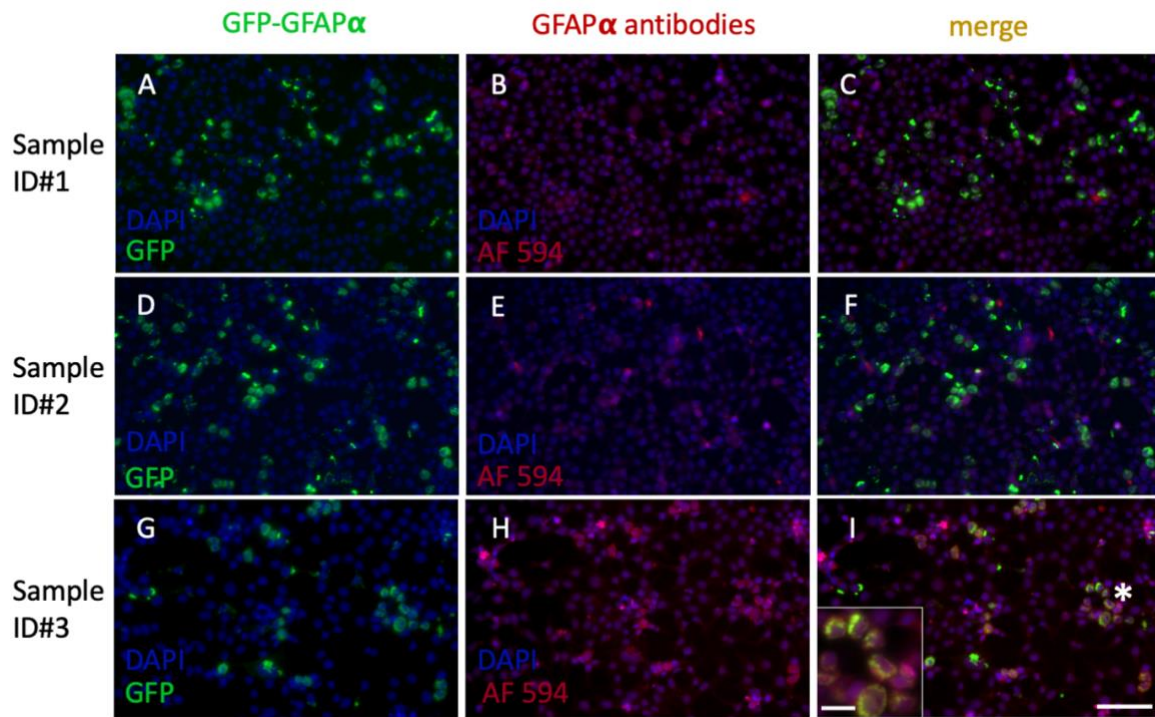
Figure 22: Screening for anti-GFAPα autoantibodies on transfected HEK293T cells in three CSF samples of an anti-GFAPα autoantibody positive patient. **(A-I)** Cell nuclei were stained with DAPI (blue). **(A, D, G)** GFP-tagged GFAPα (green) expressed in HEK293T cells is demonstrated. **(B, E, H)** Cells were immunostained with anti-GFAPα human (AF594, red). **(C, F, I)** merge images of transfected (green) and immunostained (red) cells. **(A-C/D-F)** Sample ID#1 and Sample ID#2 showed no overlap of transfected (green) and immunostained (red) cells, and were therefore anti-GFAPα IgG negative. **(G-I)** Sample ID#3 shows a light immunostaining (red) in the cells with an overlap with transfected (green) cells. Asterisk and inset in **(I)** indicates an overlap (yellow) of transfected (green) and immunostained (red) cells. Scale bar **(A-I)**: 50 μm. Scale bar **(I; Inset)**: 10 μm. CSF= cerebrospinal fluid, DAPI= 4´,6-diamidino-2-phenylindole, GFAP= glial fibrillary acidic protein, GFP= green fluorescent protein, IgG= Immunoglobulin G.

To sum up, as illustrated in **Table 6**, positive CBA and anti-neuronal TBA findings were only found in sample ID#3 from the positive patient. Sample ID#1 showed no positive anti-GFAPα IgG autoantibody staining in CBA and no signs of neuropil or astrocyte staining in anti-neuronal TBA. Sample ID#2 showed a slightly positive astrocyte staining in anti-neuronal TBA but was anti-GFAPα IgG negative.

Table 6: Overview of anti-neuronal TBA and CBA findings in anti-GFAPα IgG autoantibody positive patient.

CSF Sample ID	Date of lumbar puncture	Tissue-based assay findings	Cell-based assay findings
Sample ID#1	August 12th 2021	no signs of neuropil or astrocyte staining in the hippocampus	Anti-GFAPα IgG negative
Sample ID#2	August 17th 2021	no signs of neuropil staining, slightly positive astrocyte staining in the hippocampus	Anti-GFAPα IgG negative
Sample ID#3	August 30th 2021	incipient neuropil staining pattern in the hippocampus, radial glial staining pattern in the cerebellum	Anti-GFAPα IgG positive

CSF= cerebrospinal fluid, GFAP= glial fibrillary acidic protein, IgG= Immunoglobulin G

5 Discussion

This study was performed to search for autopsy cases with GFAP meningo-encephalomyelitis that may contribute to identify novel neuropathological patterns, clinical associations and to further expand the knowledge of the pathogenesis of this disorder. Therefore, a retrospective cohort study was carried out on patients with available autopsy tissue and CSF, serum and/or plasma samples acquired from the "Neurobiobank" from the Division of Neuropathology and Neurochemistry (NPC), Department of Neurology, Medical University of Vienna by screening all the included samples for anti-GFAPα IgG autoantibodies. In total, 450 patients were included in this study. A slight female predominance (F:M ratio=1.2:1) was found among included patients and 65% of patients were over 65 years.

A wide variety of diseases were found in included patients. The largest group with almost 50% of patients (222/450) was diagnosed with Creutzfeldt-Jakob disease (CJD). This can be explained by the fact that the NPC is the Austrian Reference Center for Prion Diseases and suspected prion cases.[1] None of these patients presented anti-GFAPα IgG autoantibodies in the fixed CBA. So far, an association of prion diseases with anti-GFAPα autoantibodies has not been described in the literature. Therefore, our data support that a correlation between CJD and GFAP meningo-encephalomyelitis is unlikely.

The second largest group with 15% of patients (66/450) was diagnosed with neurodegenerative diseases such as Alzheimer´s disease, Morbus Parkinson, argyrophilic grain disease, and Lewy-body dementia. There is only one case report describing the association between radiological, CSF and serological findings of a neurodegenerative disease (brain and spine MRI hyperintensities, atrophy and elevated levels of GFAP and neurofilaments) and anti-GFAPα autoantibodies. The authors suggested an underlying neurodegenerative mechanism in GFAP meningo-encephalomyelitis in addition to the inflammatory component [70]. Moreover, in a study of 102 patients with GFAP meningo-encephalomyelitis, dementia was described as rare clinical symptom [42, 43]. In our study, anti-GFAPα IgG autoantibodies were not detected in any of the included patients

---

[1] https://www.meduniwien.ac.at/hp/npc/allgemeine-informationen/aufgaben/oesterreichisches-referenzzentrum-zur-erfassung-und-dokumentation-menschlicher-prionen-erkrankungen-oerpe/. Access date: 02/04/2022, 12:00h

with neurodegenerative diseases. This does not support that neurodegenerative processes are a significant trigger for GFAP meningo-encephalomyelitis.

Almost 7% of patients in our autopsy cohort (30/450) were diagnosed with a primary neoplasia such as adenocarcinoma, breast cancer, Hodgkin-Lymphoma, non-Hodgkin-Lymphoma, gliofibroma, glioblastoma, meningioma and choriocarcinoma. GFAP meningo-encephalomyelitis is often accompanied by a neoplastic event, most prominently an ovarian teratoma [46]. Nevertheless, none of the patients with a primary neoplasia included in this study were detected with anti-GFAPα IgG autoantibodies, which may be due to the small sample size and/or a selection bias towards highly aggressive tumor types with short disease course or tumor types without potential to trigger anti-GFAPα autoantibodies.

Interestingly, 4% of patients (20/450) were diagnosed with an antibody-associated AIE. An overlapping syndrome of GFAP meningo-encephalomyelitis with other autoimmune diseases with anti-neuronal or anti-glial antibodies had been reported, particularly with anti-NMDAR IgG, anti-AQP4 IgG, and anti-MOG IgG [64]. These concomitant autoantibodies were found in five antibody-associated AIE patients (anti-AQP4 IgG (1/20), and anti-NMDAR IgG (2/20), anti-MOG IgG (2/20)). In addition, half of the included antibody-associated AIE patients (10/20), one of whom had anti-NMDAR IgG (1/2), were accompanied by an underlying tumor concomitant with or prior to their disorder. Nevertheless, none of the patients screened from our autopsy cohort showed anti-GFAPα IgG autoantibodies in CSF and/or serum/plasma. However, due to the small sample size of patients with antibody-associated AIE, these data cannot be assumed as representative.

Viral infections, especially HSV, were rarely discussed as possible triggers of GFAP meningo-encephalomyelitis and have been described in single case reports [51][71][50]. Viral infections occurred in 16% of our included patients (7/450), (PML (4/7), TBE (1/7), HIV (1/7), EBV (1/7)). None of these patients had anti-GFAPα IgG autoantibodies in the fixed CBA. Our findings may support that viral infection only rarely trigger GFAP meningo-encephalomyelitis but further studies with larger sample sizes are necessary to confirm this hypothesis.

In summary, a total of 599 samples such as CSF, serum, and/or plasma from 450 patients were screened for anti-GFAPα IgG autoantibodies by CBA, none of whom were tested positive. A major limitation of our study was that 22% of our included patients only had serum or plasma available for anti-GFAPα IgG autoantibody screening. A higher sensitivity

of anti-GFAPα IgG autoantibodies in CSF is described in the literature [43]. Therefore, a positive result in the CSF of these patients cannot be ruled out.

Moreover, 65% of patients in our autopsy cohort were older than 65 years, while the literature suggests a median age at disorder onset of around 45 years [2][3]. Screening of autopsy cohorts of younger patients with death before the age of 65 years might increase the probability to find positive results.

An additional project in this study analyzed, whether the TBA performed for the diagnostic screening of anti-neuronal antibodies at the NPC (anti-neuronal TBA), is a useful method to screen for anti-GFAPα autoantibodies. Therefore, 31 patients with positive astrocyte staining in the anti-neuronal TBA showing characteristic Bergmann radial staining pattern in the cerebellar cortex and astrocyte staining in the hippocampus were analyzed and screened for anti-GFAPα IgG autoantibodies in the fixed CBA. Only one out of the 31 cases showed a positive result in the CBA, while the other 30 cases remained negative. The positive case was a twenty-year-old man, who presented with a low titer of anti-GFAPα IgG autoantibodies in CBA. He initially presented symptoms suggestive for an infectious disease with negative results in viral, bacterial, and fungal screening and did not respond to antibiotic and antiviral treatment. Additionally, the patient developed clinical and radiological features of meningitis. Corticosteroid therapy showed an improvement of his clinical picture. The clinical manifestation and failure of antibiotic and antiviral treatment are consistent with the characteristics of GFAP meningo-encephalomyelitis [42]. Interestingly, a systematic screening of follow-up samples revealed that the astrocyte staining in anti-neuronal TBA and anti-GFAPα IgG autoantibodies in CBA were first detected after the meningitis developed and corticosteroids were administered. The previously administered immunotherapy could explain the low titers of anti-GFAPα IgGs.

In contrast, the other 30 samples with astrocyte staining in the anti-neuronal TBA had no anti-GFAPα IgG staining in CBA and their staining is most likely an unspecific reactivity with astrocytes. This indicates a low specificity of the anti-neuronal TBA for the screening of anti-GFAPα IgG. The establishment of a novel TBA that will be specifically used for the screening of anti-glial antibodies, using unfixed rat or mouse brains according to the modified protocol of Flanagan et al [43] will be necessary to provide a robust second detection method for the confirmation of anti-GFAPα IgG.

5.1 Conclusion

In this study we systematically screened an autopsy cohort of 450 patients with heterogenous diseases, none of whom had anti-GFAPα IgG autoantibodies. We could not identify CJD, neurodegeneration and viral infections as significant triggers for GFAP meningo-encephalomyelitis. Moreover, we could not find patients with concomitant anti-neuronal or anti-glial autoimmune diseases with anti-GFAPα IgG.

This master thesis has important limitations and may explain our negative results: (1) our autopsy cohort had a predominance in patients >65 years (65%), (2) small sample sizes in some disease cohorts (e.g., viral infections (7/450), meningo-encephalitis (6/450), meningitis (2/450), meningo-encephalomyelitis (2/450)), and (3) no CSF availability in 22% of the included patients which may produce false negative results. Since neuropathological findings in patients with anti-GFAPα IgG may help to understand pathogenic mechanisms that trigger GFAP meningo-encephalomyelitis, continuous screening for such cases in larger cohorts will be important in future.

In our second project we investigated the specificity of the anti-neuronal TBA, which is established at the NPC for the diagnostic screening of anti-neuronal surface antibodies, to screen for anti-GFAPα IgG. Only one out of 31 patients with a positive astrocyte staining pattern was confirmed to have anti-GFAPα IgG in the fixed CBA. This result indicates a low specificity of the anti-neuronal TBA for the screening of anti-GFAPα IgG and the establishment of a novel TBA, using unfixed rat or mouse brains according to the modified protocol of Flanagan et al [43], will be necessary to provide a robust second detection method for the confirmation of anti-GFAPα IgG.

In summary, many factors of GFAP meningo-encephalomyelitis are still unknown. So far the literature comprises only small case numbers from monocentric studies, therefore the epidemiology and prevalence of this disorder is hard to determine [1][46][10]. A low diagnostic rate leads to fewer detected cases and thus to a deficit in the understanding of the pathogenesis and triggers of this disorder, as well as the clinical manifestations and prognosis. Future studies with larger sample size will be necessary to elucidate the pathogenesis and possible triggers of GFAP meningo-encephalomyelitis.

6 Abstract

Background: Glial fibrillary acidic protein (GFAP) meningo-encephalomyelitis is a novel autoimmune disorder of the CNS associated with IgG autoantibodies against GFAP, an intracellular astrocytic antigen. Until now, only few monocentric case series have been described and the pathogenesis remains widely unclear.

Objectives: To search for autopsy cases with GFAP meningo-encephalomyelitis and to investigate whether the tissue-based assay optimized for anti-neuronal surface antibodies (anti-neuronal TBA) is useful to screen for anti-GFAPα autoantibodies.

Methods: Patient samples (CSF, serum and/or plasma) paired with autopsies or astrocyte-staining in the anti-neuronal TBA were screened for anti-GFAPα autoantibodies using a fixed CBA. Clinical, epidemiological, and neuropathological data were retrospectively obtained and evaluated.

Results: 599 samples of 450 patients (F:M ratio=1.2:1; <19years=2%, 19-65years=33%, >65years=65%) were screened for anti-GFAPα autoantibodies. Neuropathological diagnosis included Creutzfeldt-Jakob disease (222/450), neurodegenerative diseases (66/450), primary neoplasia (e.g., CNS tumors) (30/450), antibody-associated autoimmune encephalitis (20/450), viral infections (7/450), encephalitis (11/450), meningo-encephalitis (6/450), meningitis (2/450), meningo-encephalomyelitis (2/450) and others (85/450). None of the 599 samples were positive for anti-GFAPα autoantibodies. Subsequently, 31 patients with astrocyte-staining in the anti-neuronal TBA were screened for anti-GFAPα autoantibodies. Only one case showed a positive result in the CBA.

Conclusion: Continuous screening for anti-GFAPα autoantibodies in larger autopsy cohorts will be necessary to identify GFAP meningo-encephalomyelitis cases. The anti-neuronal TBA may show unspecific labeling of astrocytes and is therefore not useful for the screening of anti-GFAPα autoantibodies. The establishment of a novel TBA will be necessary to provide a robust second detection method for the confirmation of anti-GFAPα autoantibodies.

7 Zusammenfassung

Hintergrund: Die Saure Gliafaser Protein (glial fibrillary acidic protein; GFAP) -Meningo-enzephalomyelitis ist eine neuartige Autoimmunerkrankung des zentralen Nervensystems, die mit Autoantikörpern gegen GFAPα, einem intrazellulären Antigen in Astrozyten, einhergeht. Bisher wurden nur wenige monozentrische Fallserien beschrieben und die Pathogenese bleibt weitgehend unklar.

Ziel: Das Ziel ist es, Autopsiefälle von PatientInnen mit GFAP-Meningo-enzephalomyelitis zu identifizieren und zu untersuchen, ob der gewebsbasierte Assay (TBA), welcher für den Nachweis anti-neuronaler Antikörper etabliert wurde (antineuronaler TBA), für den Nachweis der Anti-GFAPα-IgG-Autoantikörper geeignet ist.

Methodik: Patientenproben (Liquor, Serum und/oder Plasma), von denen entweder Autopsien, oder ein TBA mit Astrozytenfärbemuster verfügbar war, wurden auf Anti-GFAPα-IgG-Autoantikörper mittels eines fixierten zell-basierten Assays untersucht. Klinische, epidemiologische und neuropathologische Daten wurden retrospektiv erhoben und ausgewertet.

Ergebnisse: 599 Proben von 450 PatientInnen (F:M-Verhältnis=1,2:1; <19Jahre=2%, 19-65Jahre=33%, >65Jahre=65%) wurden auf Anti-GFAPα-IgG-Autoantikörper untersucht. Zu den neuropathologischen Diagnosen zählten Creutzfeldt-Jakob-Krankheit (222/450), neurodegenerative Erkrankungen (66/450), primäre Tumore (z.B. Gehirntumor) (30/450), Antikörper-assoziierte Autoimmun-Enzephalitis (AIE) (20/450), Virusinfektionen (7/450), Enzephalitis (11/450), Meningo-enzephalitis (6/450), Meningitis (2/450), Meningo-enzephalomyelitis (2/450) und andere (85/450). In keiner der 599 Proben konnten Anti-GFAPα-IgG-Autoantikörper nachgewiesen werden. In einem zweiten Schritt wurden 31 PatientInnen mit positivem Astrozyten-Färbemuster im anti-neuronalen TBA auf Anti-GFAPα-IgG-Autoantikörper untersucht. Nur einer (1/31) war im zell-basierten Assay positiv.

Fazit: Kontinuierliches Screening auf Anti-GFAPα-IgG-Autoantikörper in größeren Autopsie-Kohorten wird notwendig sein, um Fälle mit GFAP-Meningo-enzephalomyelitis zu identifizieren. Aufgrund vieler unspezifisch positiver Fälle ist der anti-neuronale TBA für den Nachweis von Anti-GFAPα-IgG-Autoantikörper nicht geeignet, sodass die Etablierung eines neuen TBAs notwendig sein wird, um eine verlässliche zweite

Nachweismethode zur Bestätigung der Anti-GFAPα-IgG-Autoantikörper zur Verfügung zu haben.

8   Bibliography

[1]   A. N. Theofilopoulos, D. H. Kono, and R. Baccala, "The multiple pathways to autoimmunity," *Nat. Immunol.*, vol. 18, no. 7, pp. 716–724, Jul. 2017, doi: 10.1038/ni.3731.

[2]   G. Lu, X. Hao, W.-H. Chen, and S. Mu, "GAAD: A Gene and Autoimmiune Disease Association Database," *Genomics Proteomics Bioinformatics*, vol. 16, no. 4, pp. 252–261, Aug. 2018, doi: 10.1016/j.gpb.2018.05.001.

[3]   B. Alberts, *Molecular biology of the cell*, Sixth edition. New York, NY: Garland Science, Taylor and Francis Group, 2015.

[4]   E. Mariño and S. T. Grey, "B cells as effectors and regulators of autoimmunity," *Autoimmunity*, vol. 45, no. 5, pp. 377–387, Aug. 2012, doi: 10.3109/08916934.2012.665527.

[5]   B. Obermeier, A. Verma, and R. M. Ransohoff, "Chapter 3 - The blood–brain barrier," in *Handbook of Clinical Neurology*, vol. 133, S. J. Pittock and A. Vincent, Eds. Elsevier, 2016, pp. 39–59. doi: 10.1016/B978-0-444-63432-0.00003-7.

[6]   M. D. Sweeney, Z. Zhao, A. Montagne, A. R. Nelson, and B. V. Zlokovic, "Blood-Brain Barrier: From Physiology to Disease and Back," *Physiol. Rev.*, vol. 99, no. 1, pp. 21–78, Jan. 2019, doi: 10.1152/physrev.00050.2017.

[7]   J. Dalmau, C. Geis, and F. Graus, "Autoantibodies to Synaptic Receptors and Neuronal Cell Surface Proteins in Autoimmune Diseases of the Central Nervous System," *Physiol. Rev.*, vol. 97, no. 2, pp. 839–887, Apr. 2017, doi: 10.1152/physrev.00010.2016.

[8]   R. Höftberger, "Neuroimmunology: an expanding frontier in autoimmunity," *Front. Immunol.*, vol. 6, p. 206, 2015, doi: 10.3389/fimmu.2015.00206.

[9]   F. Graus *et al.*, "Recommended diagnostic criteria for paraneoplastic neurological syndromes," *J. Neurol. Neurosurg. Psychiatry*, vol. 75, no. 8, pp. 1135–1140, Aug. 2004, doi: 10.1136/jnnp.2003.034447.

[10]   R. Höftberger, M. R. Rosenfeld, and J. Dalmau, "Update on neurological paraneoplastic syndromes," *Curr. Opin. Oncol.*, vol. 27, no. 6, pp. 489–495, Nov. 2015, doi: 10.1097/CCO.0000000000000222.

[11]   H. Alexopoulos and M. C. Dalakas, "The immunobiology of autoimmune encephalitides," *J. Autoimmun.*, vol. 104, p. 102339, Nov. 2019, doi: 10.1016/j.jaut.2019.102339.

[12]   J. Broadley *et al.*, "Prognosticating autoimmune encephalitis: A systematic review," *J. Autoimmun.*, vol. 96, pp. 24–34, Jan. 2019, doi: 10.1016/j.jaut.2018.10.014.

[13]   C. G. Bien *et al.*, "Immunopathology of autoantibody-associated encephalitides: clues for pathogenesis," *Brain J. Neurol.*, vol. 135, no. Pt 5, pp. 1622–1638, May 2012, doi: 10.1093/brain/aws082.

[14]   M. S. Nissen, M. Ryding, M. Meyer, and M. Blaabjerg, "Autoimmune Encephalitis: Current Knowledge on Subtypes, Disease Mechanisms and Treatment," *CNS Neurol. Disord. Drug Targets*, vol. 19, no. 8, pp. 584–598, 2020, doi: 10.2174/1871527319666200708133103.

[15] F. Graus *et al.*, "Updated Diagnostic Criteria for Paraneoplastic Neurologic Syndromes," *Neurol. - Neuroimmunol. Neuroinflammation*, vol. 8, no. 4, p. e1014, Jul. 2021, doi: 10.1212/NXI.0000000000001014.

[16] J. E. Greenlee and H. R. Brashear, "Antibodies to cerebellar Purkinje cells in patients with paraneoplastic cerebellar degeneration and ovarian carcinoma," *Ann. Neurol.*, vol. 14, no. 6, pp. 609–613, Dec. 1983, doi: 10.1002/ana.410140603.

[17] F. Graus, C. Cordon-Cardo, and J. B. Posner, "Neuronal antinuclear antibody in sensory neuronopathy from lung cancer," *Neurology*, vol. 35, no. 4, pp. 538–538, Apr. 1985, doi: 10.1212/WNL.35.4.538.

[18] J. E. Greenlee, N. G. Carlson, J. R. Abbatemarco, I. Herdlevær, S. L. Clardy, and C. A. Vedeler, "Paraneoplastic and Other Autoimmune Encephalitides: Antineuronal Antibodies, T Lymphocytes, and Questions of Pathogenesis," *Front. Neurol.*, vol. 12, p. 744653, 2021, doi: 10.3389/fneur.2021.744653.

[19] L. Seluk *et al.*, "A large screen for paraneoplastic neurological autoantibodies; diagnosis and predictive values," *Clin. Immunol. Orlando Fla*, vol. 199, pp. 29–36, Feb. 2019, doi: 10.1016/j.clim.2018.12.007.

[20] D. Dubey *et al.*, "Autoimmune encephalitis epidemiology and a comparison to infectious encephalitis," *Ann. Neurol.*, vol. 83, no. 1, pp. 166–177, Jan. 2018, doi: 10.1002/ana.25131.

[21] N. Hansen and C. Timäus, "Autoimmune encephalitis with psychiatric features in adults: historical evolution and prospective challenge," *J. Neural Transm. Vienna Austria 1996*, vol. 128, no. 1, pp. 1–14, Jan. 2021, doi: 10.1007/s00702-020-02258-z.

[22] C. E. Uy, S. Binks, and S. R. Irani, "Autoimmune encephalitis: clinical spectrum and management," *Pract. Neurol.*, vol. 21, no. 5, pp. 412–423, Oct. 2021, doi: 10.1136/practneurol-2020-002567.

[23] E. Lancaster, "The Diagnosis and Treatment of Autoimmune Encephalitis," *J. Clin. Neurol. Seoul Korea*, vol. 12, no. 1, pp. 1–13, Jan. 2016, doi: 10.3988/jcn.2016.12.1.1.

[24] J. Dalmau, "NMDA receptor encephalitis and other antibody-mediated disorders of the synapse: The 2016 Cotzias Lecture," *Neurology*, vol. 87, no. 23, pp. 2471–2482, Dec. 2016, doi: 10.1212/WNL.0000000000003414.

[25] L. A. Dutra, F. Abrantes, F. F. Toso, J. L. Pedroso, O. G. P. Barsottini, and R. Hoftberger, "Autoimmune encephalitis: a review of diagnosis and treatment," *Arq. Neuropsiquiatr.*, vol. 76, no. 1, pp. 41–49, Jan. 2018, doi: 10.1590/0004-282X20170176.

[26] F. Leypoldt *et al.*, "Herpes simplex virus-1 encephalitis can trigger anti-NMDA receptor encephalitis: Case report," *Neurology*, vol. 81, no. 18, pp. 1637–1639, Oct. 2013, doi: 10.1212/WNL.0b013e3182a9f531.

[27] J. P. Stahl and A. Mailles, "Herpes simplex virus encephalitis update," *Curr. Opin. Infect. Dis.*, vol. 32, no. 3, pp. 239–243, Jun. 2019, doi: 10.1097/QCO.0000000000000554.

[28] V. Oliveira, G. Videira, R. Samões, P. Carneiro, E. Neves, and E. Santos, "Paraneoplastic neurological syndromes with onconeural antibodies: A single center retrospective study," *J. Neurol. Sci.*, vol. 418, p. 117103, Nov. 2020, doi: 10.1016/j.jns.2020.117103.

[29] J. Middeldorp and E. M. Hol, "GFAP in health and disease," *Prog. Neurobiol.*, vol. 93, no. 3, pp. 421–443, Mar. 2011, doi: 10.1016/j.pneurobio.2011.01.005.

[30] B. Zhou, Y. Zuo, and R. Jiang, "Astrocyte morphology: Diversity, plasticity, and role in neurological diseases," *CNS Neurosci. Ther.*, vol. 25, no. 6, pp. 665–673, Jun. 2019,

doi: 10.1111/cns.13123.

[31]   F. Vasile, E. Dossi, and N. Rouach, "Human astrocytes: structure and functions in the healthy brain," *Brain Struct. Funct.*, vol. 222, no. 5, pp. 2017–2029, Jul. 2017, doi: 10.1007/s00429-017-1383-5.

[32]   M. F. Bear, B. W. Connors, and M. A. Paradiso, *Neuroscience: exploring the brain*, 4. ed. Philadelphia: Wolters Kluwer, 2016.

[33]   V. Gallo and B. Deneen, "Glial development: the crossroads of regeneration and repair in the CNS," *Neuron*, vol. 83, no. 2, pp. 283–308, Jul. 2014, doi: 10.1016/j.neuron.2014.06.010.

[34]   A. V. Molofsky *et al.*, "Astrocytes and disease: a neurodevelopmental perspective," *Genes Dev.*, vol. 26, no. 9, pp. 891–907, May 2012, doi: 10.1101/gad.188326.112.

[35]   D. Li *et al.*, "Neurochemical regulation of the expression and function of glial fibrillary acidic protein in astrocytes," *Glia*, vol. 68, no. 5, pp. 878–897, May 2020, doi: 10.1002/glia.23734.

[36]   M. Bradl and H. Lassmann, "Experimental Models of Neuromyelitis Optica," *Brain Pathol.*, vol. 24, no. 1, pp. 74–82, Jan. 2014, doi: 10.1111/bpa.12098.

[37]   S. Huda, D. Whittam, M. Bhojak, J. Chamberlain, C. Noonan, and A. Jacob, "Neuromyelitis optica spectrum disorders," *Clin. Med. Lond. Engl.*, vol. 19, no. 2, pp. 169–176, Mar. 2019, doi: 10.7861/clinmedicine.19-2-169.

[38]   S. Jarius, F. Paul, B. G. Weinshenker, M. Levy, H. J. Kim, and B. Wildemann, "Neuromyelitis optica," *Nat. Rev. Dis. Primer*, vol. 6, no. 1, p. 85, Oct. 2020, doi: 10.1038/s41572-020-0214-9.

[39]   C. F. Lucchinetti, Y. Guo, B. F. Gh. Popescu, K. Fujihara, Y. Itoyama, and T. Misu, "The Pathology of an Autoimmune Astrocytopathy: Lessons Learned from Neuromyelitis Optica: Autoimmune Astrocytopathy," *Brain Pathol.*, vol. 24, no. 1, pp. 83–97, Jan. 2014, doi: 10.1111/bpa.12099.

[40]   A. Sosunov, M. Olabarria, and J. E. Goldman, "Alexander disease: an astrocytopathy that produces a leukodystrophy," *Brain Pathol. Zurich Switz.*, vol. 28, no. 3, pp. 388–398, May 2018, doi: 10.1111/bpa.12601.

[41]   B. Fang *et al.*, "Autoimmune Glial Fibrillary Acidic Protein Astrocytopathy: A Novel Meningoencephalomyelitis," *JAMA Neurol.*, vol. 73, no. 11, pp. 1297–1307, Nov. 2016, doi: 10.1001/jamaneurol.2016.2549.

[42]   F. Shan, Y. Long, and W. Qiu, "Autoimmune Glial Fibrillary Acidic Protein Astrocytopathy: A Review of the Literature," *Front. Immunol.*, vol. 9, p. 2802, 2018, doi: 10.3389/fimmu.2018.02802.

[43]   E. P. Flanagan *et al.*, "Glial fibrillary acidic protein immunoglobulin G as biomarker of autoimmune astrocytopathy: Analysis of 102 patients," *Ann. Neurol.*, vol. 81, no. 2, pp. 298–309, Feb. 2017, doi: 10.1002/ana.24881.

[44]   A. Zekeridou, A. McKeon, and E. P. Flanagan, "A path to understanding autoimmune astrocytopathy," *Eur. J. Neurol.*, vol. 25, no. 3, pp. 421–422, Mar. 2018, doi: 10.1111/ene.13527.

[45]   A. Kimura, M. Takemura, Y. Yamamoto, Y. Hayashi, K. Saito, and T. Shimohata, "Cytokines and biological markers in autoimmune GFAP astrocytopathy: The potential role for pathogenesis and therapeutic implications," *J. Neuroimmunol.*, vol. 334, p. 576999, Sep. 2019, doi: 10.1016/j.jneuroim.2019.576999.

[46]   J. Xiao *et al.*, "Clinical, neuroradiological, diagnostic and prognostic profile of

autoimmune glial fibrillary acidic protein astrocytopathy: A pooled analysis of 324 cases from published data and a single-center retrospective study," *J. Neuroimmunol.*, vol. 360, p. 577718, Nov. 2021, doi: 10.1016/j.jneuroim.2021.577718.

[47]   A. Kunchok, A. Zekeridou, and A. McKeon, "Autoimmune glial fibrillary acidic protein astrocytopathy," *Curr. Opin. Neurol.*, vol. 32, no. 3, pp. 452–458, Jun. 2019, doi: 10.1097/WCO.0000000000000676.

[48]   X. Yang *et al.*, "Astrocytic damage in glial fibrillary acidic protein astrocytopathy during initial attack," *Mult. Scler. Relat. Disord.*, vol. 29, pp. 94–99, Apr. 2019, doi: 10.1016/j.msard.2019.01.036.

[49]   E.-S. Park, K. Uchida, and H. Nakayama, "Establishment of a Rat Model for Canine Necrotizing Meningoencephalitis (NME)," *Vet. Pathol.*, vol. 51, no. 6, pp. 1151–1164, Nov. 2014, doi: 10.1177/0300985813519115.

[50]   J. Li, Y. Xu, H. Ren, Y. Zhu, B. Peng, and L. Cui, "Autoimmune GFAP astrocytopathy after viral encephalitis: A case report," *Mult. Scler. Relat. Disord.*, vol. 21, pp. 84–87, Apr. 2018, doi: 10.1016/j.msard.2018.02.020.

[51]   M. Handoko, W. Hong, E. Espineli, K. Saxena, E. Muscal, and S. Risen, "Autoimmune Glial Fibrillary Acidic Protein Astrocytopathy Following Herpes Simplex Virus Encephalitis in a Pediatric Patient," *Pediatr. Neurol.*, vol. 98, pp. 85–86, Sep. 2019, doi: 10.1016/j.pediatrneurol.2019.05.010.

[52]   Divyanshu Dubey *et al.*, "Autoimmune GFAP astrocytopathy: Prospective evaluation of 90 patients in 1 year," *J. Neuroimmunol.*, vol. 321, pp. 157–163, Aug. 2018, doi: 10.1016/j.jneuroim.2018.04.016.

[53]   A. G. Dumonceau *et al.*, "Glial Fibrillary Acidic Protein Autoimmunity: A French Cohort Study," *Neurology*, p. 10.1212/WNL.0000000000013087, Nov. 2021, doi: 10.1212/WNL.0000000000013087.

[54]   R. Iorio *et al.*, "Clinical and immunological characteristics of the spectrum of GFAP autoimmunity: a case series of 22 patients," *J. Neurol. Neurosurg. Psychiatry*, vol. 89, no. 2, pp. 138–146, Feb. 2018, doi: 10.1136/jnnp-2017-316583.

[55]   Y. Long *et al.*, "Autoimmune glial fibrillary acidic protein astrocytopathy in Chinese patients: a retrospective study," *Eur. J. Neurol.*, vol. 25, no. 3, pp. 477–483, Mar. 2018, doi: 10.1111/ene.13531.

[56]   V. Oger *et al.*, "Mild Encephalitis/Encephalopathy with reversible splenial lesion syndrome: An unusual presentation of anti-GFAP astrocytopathy," *Eur. J. Paediatr. Neurol.*, vol. 26, pp. 89–91, May 2020, doi: 10.1016/j.ejpn.2020.03.002.

[57]   M. Yamakawa, K. O. Hogan, J. Leever, and Y. N. Jassam, "Autopsy Case of Meningoencephalomyelitis Associated With Glial Fibrillary Acidic Protein Antibody," *Neurol. - Neuroimmunol. Neuroinflammation*, vol. 8, no. 6, p. e1081, Nov. 2021, doi: 10.1212/NXI.0000000000001081.

[58]   Y. Shu *et al.*, "Brain Immunohistopathology in a Patient with Autoimmune Glial Fibrillary Acidic Protein Astrocytopathy," *Neuroimmunomodulation*, vol. 25, no. 1, pp. 1–6, 2018, doi: 10.1159/000488879.

[59]   X. Yang *et al.*, "Overlapping Autoimmune Syndromes in Patients With Glial Fibrillary Acidic Protein Antibodies," *Front. Neurol.*, vol. 9, p. 251, Apr. 2018, doi: 10.3389/fneur.2018.00251.

[60]   M. Guasp and J. Dalmau, "Encephalitis associated with antibodies against the NMDA receptor," *Med. Clínica Engl. Ed.*, vol. 151, no. 2, pp. 71–79, Jul. 2018, doi:

10.1016/j.medcle.2018.05.020.

[61]   A. L. Martin, E. Jolliffe, and S. P. Hertweck, "Ovarian Teratoma Associated with Coexisting Anti-N-Methyl-D-Aspartate Receptor and Glial Fibrillary Acidic Protein Autoimmune Meningoencephalitis in an Adolescent Girl: A Case Report," *J. Pediatr. Adolesc. Gynecol.*, vol. 31, no. 3, pp. 321–324, Jun. 2018, doi: 10.1016/j.jpag.2017.12.009.

[62]   H. Ikeshima-Kataoka, "Neuroimmunological Implications of AQP4 in Astrocytes," *Int. J. Mol. Sci.*, vol. 17, no. 8, p. E1306, Aug. 2016, doi: 10.3390/ijms17081306.

[63]   Y. Wu, L. Zhong, and J. Geng, "Neuromyelitis optica spectrum disorder: Pathogenesis, treatment, and experimental models," *Mult. Scler. Relat. Disord.*, vol. 27, pp. 412–418, Jan. 2019, doi: 10.1016/j.msard.2018.12.002.

[64]   H. Lin *et al.*, "Overlapping Clinical Syndromes in Patients with Glial Fibrillary Acidic Protein IgG," *Neuroimmunomodulation*, vol. 27, no. 1, pp. 69–74, 2020, doi: 10.1159/000505730.

[65]   S. Salama, M. Khan, S. Pardo, I. Izbudak, and M. Levy, "MOG antibody-associated encephalomyelitis/encephalitis," *Mult. Scler. Houndmills Basingstoke Engl.*, vol. 25, no. 11, pp. 1427–1433, Oct. 2019, doi: 10.1177/1352458519837705.

[66]   J. Ding *et al.*, "Overlapping syndrome of MOG-IgG-associated disease and autoimmune GFAP astrocytopathy," *J. Neurol.*, vol. 267, no. 9, pp. 2589–2593, Sep. 2020, doi: 10.1007/s00415-020-09869-2.

[67]   X. Yang *et al.*, "Treatment of Autoimmune Glial Fibrillary Acidic Protein Astrocytopathy: Follow-Up in 7 Cases," *Neuroimmunomodulation*, vol. 24, no. 2, pp. 113–119, 2017, doi: 10.1159/000479948.

[68]   H. Wang *et al.*, "Autoimmune glial fibrillary acidic protein astrocytopathy manifesting as subacute meningoencephalitis with descending myelitis: a case report," *BMC Neurol.*, vol. 20, no. 1, p. 443, Dec. 2020, doi: 10.1186/s12883-020-02021-7.

[69]   G. Ricken *et al.*, "Detection Methods for Autoantibodies in Suspected Autoimmune Encephalitis," *Front. Neurol.*, vol. 9, p. 841, 2018, doi: 10.3389/fneur.2018.00841.

[70]   A. Papa *et al.*, "Black holes and high levels of neurofilaments in glial fibrillary acidic protein - astrocytopathy: a case report," *Eur. J. Neurol.*, vol. 27, no. 11, pp. 2381–2384, Nov. 2020, doi: 10.1111/ene.14244.

[71]   H. So, T. Ohashi, S. Yamagishi, H. Mori, and J. Takanashi, "Case of autoimmune glial fibrillary acidic protein astrocytopathy associated with Epstein–Barr virus reactivation," *Clin. Exp. Neuroimmunol.*, p. cen3.12659, Jul. 2021, doi: 10.1111/cen3.12659.

9 List of tables

10 List of figures